Bull. Min. Res. Exp. (2017) 155: 1-31

Bulletin of the Mineral Research and Exploration

http://bulletin.mta.gov.tr

THE GEOLOGICAL EVOLUTION OF SORGUN (YOZGAT)-YILDIZELİ (SİVAS) FORELAND BASIN, PETROGRAPHIC, GEOCHEMICAL ASPECTS AND GEOCHRONOLOGY OF VOLCANISM AFFECTING THE BASIN

Ali Ekber AKÇAY[a*] and Metin BEYAZPİRİNÇ[b]

[a] *General Directorate of Mineral Research and Exploration, Department of Geology, Ankara orcid.org/0000-0002-0771-444X*
[b] *General Directorate of Mineral Research and Exploration, Department of Geology Ankara orcid.org/0000-0001-7907-5977*

Research Article

Keywords:
Sorgun-Yıldızeli foreland basin, Slab breakoff, Subduction and collision-related volcanism, Geochemistry, $^{40}Ar/^{39}Ar$ Geochronologic dating.

ABSTRACT

Sorgun-Yıldızeli basin is an east-west trending asymmetric marginal foreland (peripheral foreland basin) formed as a result of the consumption of oceanic crust of the northern branch of Neotethys due to the collision of Sakarya continent in the north and Kırşehir Block in the south. It provides much information about the geodynamic evolution of the region. The basement of the study area consists of Late Palaeozoic-Mesozoic Akdağmadeni Massif. Akdağmadeni Massif was intruded by Cenomanian-Maastrichtian granitoids and is overlain tectonically by Late Cretaceous Artova ophiolitic melange within the İzmir-Ankara-Erzincan suture zone and by Cenomanian-Maastrichtian Darmik Formation. The volcano-sedimentary sequence deposited in Sorgun-Yıldızeli foreland basin developed on the relicts of the İzmir-Ankara-Erzincan Suture Zone along the northern margin of Kırşehir Block and was named the Boğazköy Formation. The pelitic, clastic and coarse clastic levels of Upper Palaeocene-Middle Eocene Boğazköy Formation including İzmir-Ankara-Erzincan Suture Zone slices and olistostromes are differentiated as the Dolak member. Toward the inner part of the basin, a turbiditic sequence of conglomerate, sandstone, claystone including rare limestone beds was deposited, consisting of conglomerate, sandstone, claystone, rarely limestone and alternations of three different volcanic rocks (acidic, basic and intermediate) related to subduction and/or collision. Calc-alkaline lava and pyroclastics of basaltic and basalt-andesite composition were differentiated as the Pazarcık volcanic member, with lava and pyroclastics of dacitic and rhyolitic composition called the Sarayözü volcanic member and calc-alkaline lava and pyroclastics of andesitic, trachyandesitic and dacitic composition called Kiremitlik volcanic member in Sorgun-Yıldızeli basin. According to the $^{40}Ar/^{39}Ar$ geochronologic method, the ages of 57.2±2.0 Ma and 56.7±1.8 Ma were obtained for Pazarcık volcanics, 48.8±1.5 Ma for Sarayözü volcanics and 45.1±1.3 Ma and 47.3±0.6 Ma for Kiremitlik volcanics. The reefal limestones which are not thick and occur in higher parts of the Boğazköy Formation were called the Limestone member. The uppermost section of the sequence which consists of generally clastic and coarse clastics is named the Konacı member. When the sedimentation and volcanism continued in the basin, gabbroic intrusions occurred as sills and laccoliths cutting the Boğazköy Formation. These gabbroic rocks were named the Yaycılar Gabbro. The age of 51.0 ± 0.7 Ma was found for the Yaycılar Gabbro with the $^{40}Ar/^{39}Ar$ geochronologic method. As a result of slab breakoff, the relicts of the consumed oceanic crust and the released massif were uplifted rapidly and the units of Middle-Late Eocene Tokuş Formation were deposited transgressively on the Boğazköy Formation and on outcropping basement rocks in the basin which was controlled by an extensional tectonic regime. Upper Miocene-Pliocene (İncesu Formation), Pliocene and Quaternary terrestrial sediments were deposited unconformably on all older units.

Received Date: 15.12.2016
Accepted Date: 14.09.2017

1. Introduction

Significant portions of the Tertiary basins in Turkey are related to arcs, foreland basins and post-collisional basins. Arc-related basins and foreland basins have been linked to the closure of the Neo-Tethys Ocean (Görür et al., 1997).

The majority of basins forming during and after the continental collision along the Izmir-Ankara-

* *Corresponding author: Ali Ekber AKÇAY, aliekber.akcay@mta.gov.tr*
http://dx.doi.org/DOI: 10.19111/bulletinofmre.336625

Erzincan Suture Zone between the Anatolide-Tauride and Pontide tectonic units (Figure 1) (Ketin, 1966) are filled with volcano-sedimentary rocks. While post-collisional basins are widespread on the Anatolide-Tauride and Pontide tectonic units, foreland basins generally have east-west trends between the southern margin of İzmir-Ankara-Erzincan Suture Zone and Anatolide-Tauride and Kırşehir Blocks.

The volcanic rocks in these basins have been studied by many researchers (for example; Armutlu Peninsula: Genç and Yılmaz, 1997; Ercan et al., 1998; Biga Peninsula: Ercan et al., 1990, 1995; Genç, 1998; Genç et al., 2004; Dönmez et al., 2005; around Gümüşhane: Tokel, 1972; Arslan and Aliyazıcıoğlu, 2001; around Ordu: Terzioğlu, 1984; around Kastamonu: Peccerillo and Taylor, 1976; around Kargı: Yılmaz and Tüysüz, 1984; around Taşova-Amasya: Alpaslan and Terzioğlu, 1998; around Çankırı and Çorum: Tüysüz and Dellaloğlu, 1992; around Amasya-Çorum: Keskin et al., 2008; Atakay Gündoğdu, 2009; around Yozgat: Büyükönal, 1985; Tiryaki and Ekici, 2012; around Tokat-Sivas: Yılmaz et al., 1994; around Yıldızeli-Akdağmadeni: Alpaslan, 2000; Koçbulut et al., 2001). Yılmaz et al. (1997), Akçay et al. (2008) and Dalkılıç et al. (2008) produced a 1/100.000 scale geologic map covering the region of the study area.

There are two different opinions relating to tectonic environment and origin of Middle Eocene magmatic rocks cropping out in broad areas of the Anatolide-Tauride and Pontide tectonic units. According to the first view, Eocene magmatism formed in a magmatic arc environment (e.g.; Peccerillo and Taylor, 1976; Yılmaz et al., 1981; Yılmaz and Tüysüz 1984; Okay and Satır, 2006; Ustaömer et al., 2009). According to the second view, these magmatic rocks formed linked to post-collisional events following the collision of the Anatolide and Pontide tectonic units (Genç and Yılmaz, 1997; Genç et al., 2005; Tüysüz and Dellaloğlu, 1992; Yılmaz et al., 1993; Terzioğlu, 1984; Alpaslan and Terzioğlu, 1998; Alpaslan, 2000; Tüysüz et al., 1995; Koçbulut et al., 2001; Tiryaki and Ekici, 2012; Aldanmaz et al., 2000; Köprübaşı and Aldanmaz, 2004; Altunkaynak, 2007; Keskin et al., 2004, 2008; Yılmaz et al., 2001; Altunkaynak and Dilek, 2013; Gülmez et al., 2013). Keskin et al. (2004) proposed slab-breakoff as an alternative model for formation of Middle Eocene volcano-sedimentary units. This model was later adapted by other researchers for Eocene magmatism in western and north-western Turkey (e.g., Köprübaşı and Aldanmaz, 2004; Altunkaynak and Dilek, 2006; Altunkaynak, 2007; Genç and Altunkaynak, 2007; Gülmez et al., 2013).

It is difficult to distinguish volcanic rocks retaining subduction signatures (subduction, collision, post-collision) from each other using only geochemical data. Thus, determining the geodynamic processes leading to the formation of studied basins will help to reveal the origin and the source characteristics of the volcanism. The study area that is located between Sorgun (Yozgat) and Yıldızeli (Sivas) is bounded to the north by ophiolitic rocks and to the south by metamorphic rocks of the Akdağmadeni Massif (Figure 1). It includes volcano-sedimentary units representing both a foreland basin developing linked to subduction and collision in the Late Palaeocene-Early Lutetian period and to post-collisional basins which began opening in the Middle Eocene. In previous studies, these basins in the study area have not been distinguished, although the tectonic setting and the origin of Lower Tertiary volcanic rocks cropping out in the region were interpreted through post-collisional basin model. This study mapped these basins developing due to different geodynamic processes in detail, and aimed to determine the geodynamic evolution of the basin by determining stratigraphic, sedimentologic, petrography, geochemical and geochronological properties of units comprising the basin fill.

2. Regional Geology

The study area located south of the Central Pontides encompasses the İzmir-Ankara-Erzincan Suture (IAESZ) (Şengör and Yılmaz, 1981) and the northern edge of the Kırşehir Block (Figure 1).

The İzmir-Ankara-Erzincan Suture Zone comprising accretionary wedge and ensimatic island arc units separates the Sakarya continent to the north from the Kırşehir Block to the south (Figure 1).

Tüysüz and Dellaloğlu (1992) and Tüysüz et al. (1995) proposed that consumption of the oceanic crust belonging to the northern branch of Neotethys occurred in two different subduction events. The first was an ensialic arc on the Sakarya continent, whereas the other produced an ensimatic island arc with intra-oceanic subduction.

The metamorphic, ophiolitic and plutonic rocks forming the Kırşehir Block in the south have been named by different names such as the Kırşehir

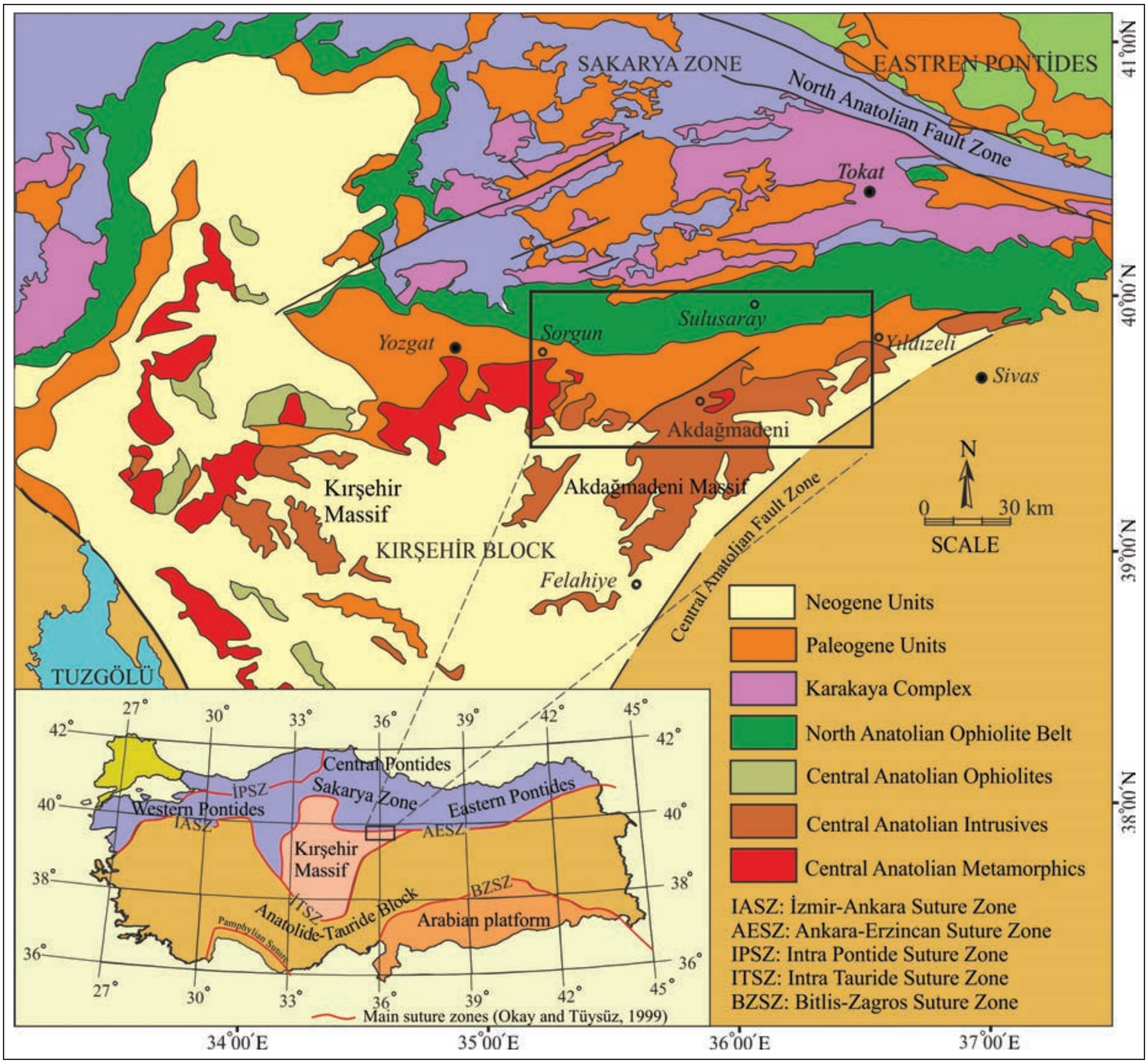

Figure 1- Location map of the study area.

crystalline massif (Bailey and McCallien, 1950, Egeran and Lahn, 1951), Central Anatolian massif, Kızılırmak Massif (Ketin, 1955, 1963; Erkan and Ataman, 1981), Central Anatolian Crystalline Melange, (Göncüoğlu et al., 1991, 1992) and the Central Anatolian Crystalline Complex (Erler and Bayhan, 1995). The same rock units are locally known as the Kırşehir Massif (Egeran and Lahn 1951), Akdağ Massif (Vache, 1963) and Niğde Massif (Göncüoğlu, 1977; Whitney et al., 2003). In this study, the name Akdağmadeni Massif (Şahin, 1999) has been adopted. This tectonic unit comprises Late Palaeozoic-Mesozoic-aged calcschist, quartzite, quartzschist, amphibole schist, amphibolite, gneiss, marble and dolomitic marble. The units generally have undergone greenschist to amphibolite facies metamorphism but the lower levels experienced higher degrees of metamorphism (Yılmaz et al., 1995).

The metamorphic rocks of the Akdağmadeni Massif (Figure 2) are commonly cut by Cenomanian-Maastrichtian-age granitoid rocks (Central Anatolian Granitoids; Erler and Bayhan, 1995). The Central Anatolian granitoids consist mainly of granite, granodiorite, syenite, microgranite, granite porphyry, monzonite and tonalite. There are skarn zones and Pb-Zn mineralizations along intrusive contacts with metamorphic rocks.

The Akdağmadeni Massif is tectonically overlain by the Late Cretaceous Artova ophiolitic melange (Özcan et al., 1980) of IAESZ and the Cenomanian-Maastrichtian Darmik Formation (Akçay et al., 2008; Dalkılıç et al., 2008) (Figure 2). The Artova ophiolitic melange comprises serpentinized peridotite, dunite, harzburgite, gabbro, diabase, pyroxenite dikes, pillow

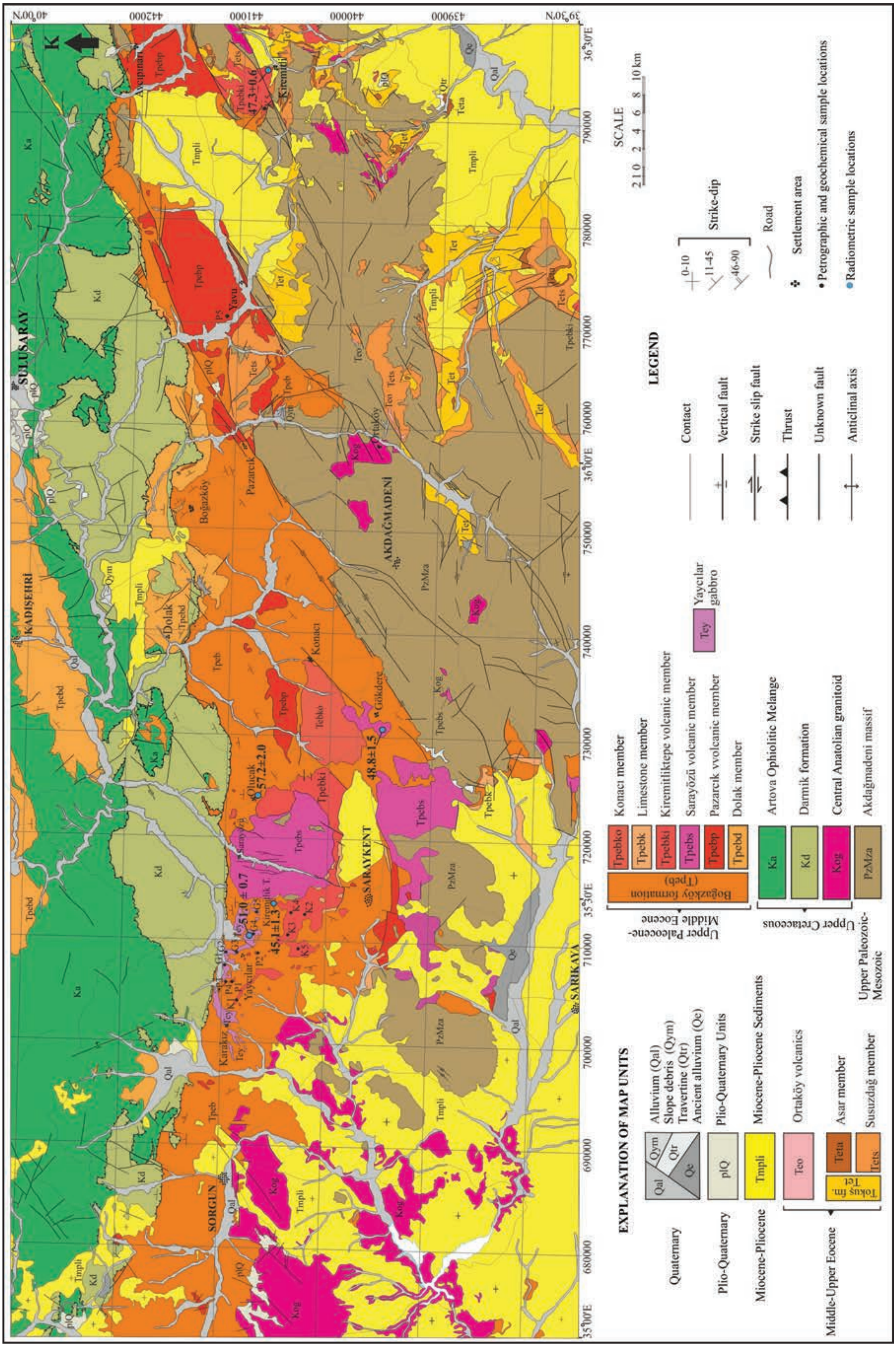

Figure 2- Geologic Map of the study.

lavas, deep sea sedimentary rocks (radiolarian chert, mudstone, calciturbidites) lacking primary textures, along with metamorphic rocks of the Sakarya continent and Triassic to Cretaceous-aged limestone slices and blocks. Late Tithonian-Berriasian and late Albian-early Cenomanian ages have been obtained from ephiophiolitic sediments within the Artova ophiolitic melange (Beyazpirinç et al., 2014). Previous studies have obtained ages of 179±15 Ma (Dilek and Thy, 2006) and 180 My (Sarıfakıoğlu et al., 2011) from plagiogranites of the ophiolitic series. According to these data, the age of oceanic crust consumed by subduction was Jurassic-Cretaceous. The Darmik Formation (Figure 3), following the Artova ophiolitic melange with a tectonic contact, consists of basaltic and andesitic lava and pyroclastic deposits in the lower levels with conglomerate, sandstone, claystone, mudstone, clayey limestone, micritic limestones and calciturbidites with volcanic interlayers in the upper sections. Beyazpirinç et al. (2014) determined the following fossils in claystone, mudstone, clayey limestone and micritic limestons in the upper sections of the Darmik Formation and identified the age as Santonian-Maastrichtian according to these fossil assemblages. Santonian: *Marginotruncana coronata* Bolli, *Marginotruncana* cf. *tarfayaensis* (Lehmann), *Marginotruncana pseudolinneiana* Pessagno, *Dicarinella* cf. *asymetrica* (Sigal), *Dicarinella concovata* (Brotzen), *Globigerinelloides* sp., *Heterohelix* sp., *Marginotruncana* sp. fossil assemblages.

Santonian-Early Maastrichtian: *Globotruncana bulloides* Vogler, *Globotruncana* cf. *arca* (Cushman), *Globotruncana* cf. *linneiana* (d'Orbigny), *Globotruncana* sp., *Globotruncanita* sp., *Heterohelix* sp. fossil assemblage.

Campanian-Maastrichtian: *Reinhardtites levis* Prins ve Sissingh, *Micula swastica* Stradner ve Steinmetz, *Arkhangelskiella cymbiformis* Vekshina, *Lucianorhabus cayeuxii* Deflandre, *Quadrum gothicum* (Deflandre), *Prediscosphaera cretacea* (Arkhangelsky), *Tranolithus phacelosus* Stover, *Micula decussata* Vekshina, *Microrhabdulus decoratus* Deflandre, *Cretarhabdus crenulatus* Bramlette ve Martini, *Watznaueria barnesae* (Black, Black ve Barnes), *Biscutum* sp. nanno fossil assemblage.

An age of 98.7±2.4 Ma ($^{40}Ar/^{39}Ar$; plagioclase) has been obtained from the volcanic rocks of the Darmik Formation. When the palaeontologic and geochronologic data are assessed together, it is observed that the Darmik Formation formed during the Cenomani-Maastrichtian period (Beyazpirinç et al., 2014).

The Late Palaeocene-Middle Eocene Boğazköy Formation that is composed of volcano-sedimentary rocks unconformably overlies the units mentioned above. The basal sections of the Boğazköy Formation comprise gabbroic rocks emplaced as sills and laccoliths, called the Yaycılar gabbro (Figure 3). The Middle-Late Eocene-aged Tokuş Formation (Yılmaz, 1982) overlies the Boğazköy Formation and basement rocks with an unconformity. In this study, basal conglomerates (Yılmaz et al., 1995) and the sandstone, claystone, fossiliferous limestone (Yılmaz et al., 1995) of Tokuş Formation are distinguished as Susuzdağ member and Asar member, respectively (Figure 3).

The Susuzdağ member is represented by reddish-brown, grey, poorly sorted conglomerate, sandstone and mudstone representing alluvial fan, fan-delta and fluvial sediments. The Asar member is yellowish-grey, cream, and yellow colour, has massive-thick bedded layers with dissolution cavities with pebble, and consists of sand and clay in the basal sections and fossiliferous limestone in the upper sections. Samples obtained from different levels in the Asar member have obtained *Discocyclina* sp., *Sphaerogypsina* sp., *Lockhartia* sp., *Asterigerina* sp., *Nummulites* sp., *Nummulites* spp., *Assilina* spp., *Nummulites* gr. *perforatus* (Montfort), *Nummulites* sp., *Orbitolites* sp., *Alveolina* sp., *Rotalia* sp., *Gypsina* sp., *Haymanaella* sp., *Nummulites* gr. *perforatus* (De Montfort), *Nummulites* cf. *perforatus* (De Montfort), *Gyroidinella magna* Le Calvez, *Linderina brugesi* Schlumberger, *Assilina* cf. *exponens* (Sowerby), *Alveolina* gr. *fusiformis* (Sowerby), *Alveolina* cf. *fusiformis* (Sowerby), *Glomalveolina* sp., *Assilina* sp., Rotaliidae, Textulariidae, Miliolidae algae, bryozoans, gastropods and macro shell fragments for a Late Lutetian-Bartonian age. However, according to a fossil assemblage including *Orbitolites complantus* Lamack, *Assilina exponens* (Sowerby), *Assilina* cf. *spira* (de Roissy), *Nummulites* cf. *millecaput* (Boubee), *Nummulites* cf. *helveticus* Kaufmann, and *Locharia cushmani* Applin et Jordan (Yılmaz et al., 1995) within the unit, however, the age of the unit is Lutetian-Priabonian. As a result, the age of the Tokuş Formation can be said to be Middle-Upper Eocene.

The acidic lava and pyroclastic rocks interfingering with the basal conglomerates (Susuzdağ member) of the Tokuş Formation around Ortaköy are named as the

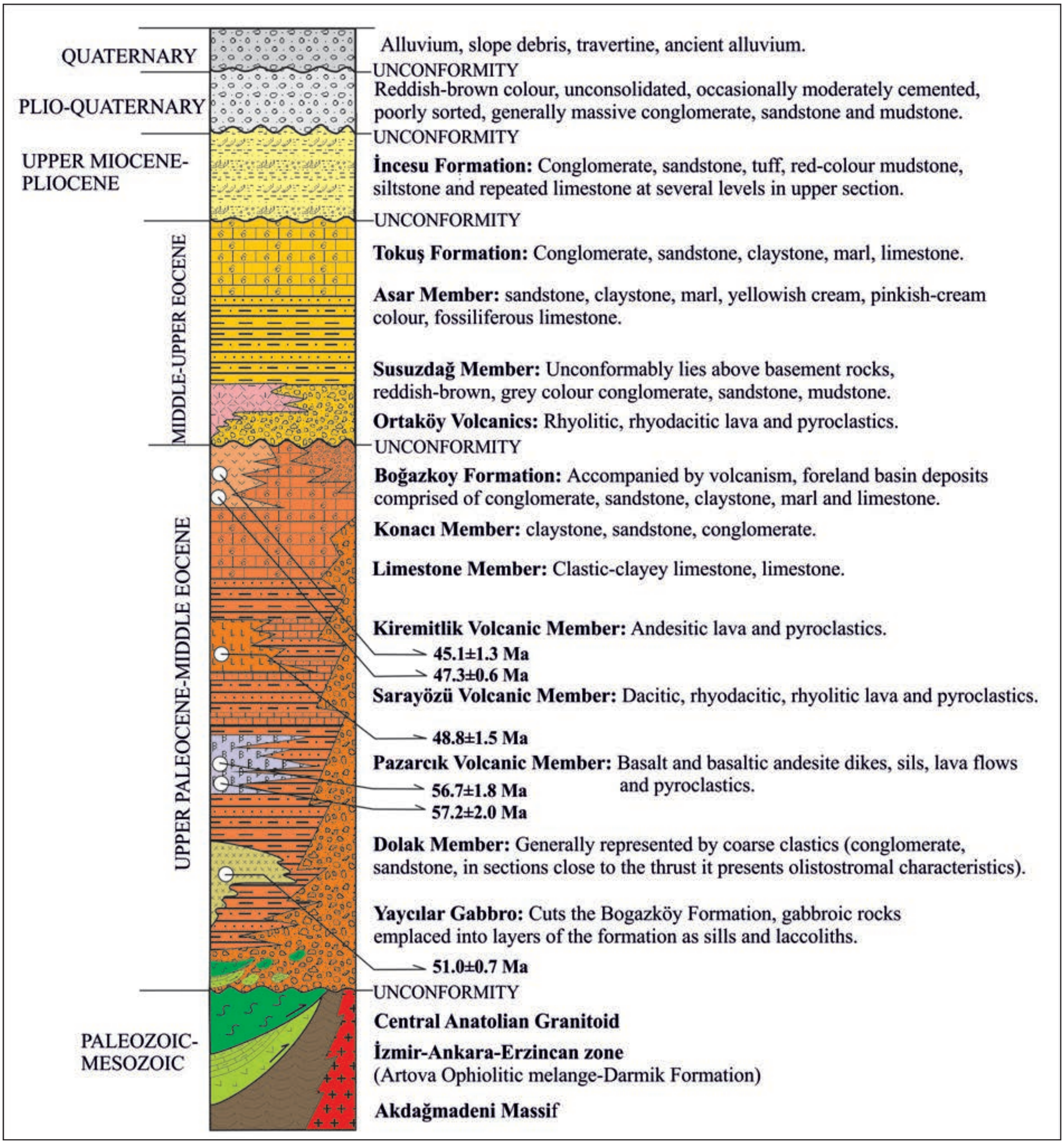

Figure 3- Generalized stratigraphic section of the study area (no scale).

Ortaköy volcanics in this study (Figures 2, 3). The unit is represented by yellowish, light grey colour rhyolite and rhyodacite lava and pyroclastic rocks. Yılmaz et al. (1995) called the unit the Ortaköy tuff and stated that even though it appears to interfinger with the Eocene-age Susuzdağ member, it may be younger.

Above this whole sequence, an angular unconformity is overlain by alluvial fan, loosely consolidated conglomerate, sandstone, tuff, red coloured mudstone, and siltstone deposited in a braided fluvial and lacustrine environment with several repeated levels of carbonate sediments in upper levels called the the Late Miocene-Pliocene İncesu Formation (Yılmaz, 1981). Based upon the presence of fossils e.g. o *Cyprideis* cf. *vetroundulate* Kırstıc, *Cyprideis torosa* Jones, *Cyprideis tuberculata* (Mehes), *Jlyocypris gibba*, *Hypraion gracile* Kaup, lower molar teeth belonging to *Choerolophodon Pentelici*, bone and tooth pieces belonging to *Proboscidae* (elephants) order, and pollen such as *Monoporollenites solaris*, *Pityosporites microalatus*, *Periporopollenites multiparatus* obtained from various locations of the unit, the age is Late Miocene-Pliocene (Kara, 1997).

The İncesu Formation is unconformably overlain by Plio-Quaternary units. The Plio-Quaternary sedimentary rocks are reddish-brown colour, poorly to moderately consolidated, poorly sorted, and comprise generally massive conglomerate, sandstones and mudstone. They generally contain the rock fragments derived from the underlying sedimentary rocks. The youngest sediments in the study area are represented by alluvium (Qal), ancient alluvium (Qe), slope debris (Qym) and travertine sediments.

3. Material and Methods

A detailed geological map was produced for the study area between Sorgun-Yıldızeli covering the 1/100.000 scale Yozgat I34, I35 and Sivas I36 sheets. Where necessary, areas outside the study area were visited in order to make correlations and observations. Thin sections were prepared from 58 hand samples collected from the study area and investigated in detail with a polarising microscope and petrographic identification performed. The great majority of volcanic rocks cropping out in the study area have been affected by alteration. A total of 17 samples chosen during field studies and petrographic investigations were sent to Canada ACME Labs for analysis (major, trace and rare earth elements). At the laboratory, these samples were ground to powder and then 0.2 g fractions were mixed with 1.5 g $Li\text{-}BO_2$ and heated to 105°C. The hot mixture and 100 ml 5% HNO_3 were mixed and the solution was evaporated in an ICP-ES (inductively coupled plasma emission spectrometer) to identify major element oxides and trace elements. The detection limit for major element oxides was 0.002-0.04%. For rare earth element (REE) analysis, samples prepared with the methods above were placed in an ICP-MS (inductively coupled plasma mass spectrometer). The trace element detection limit was between 0.01 and 5 ppm.

In order to determine the radiometric ages, a total of 6 samples - 2 samples from the Pazarcık volcanic member, 1 sample from the Sarayözü volcanic member, 2 samples from the Kiremitlik volcanic member and 1 sample from the Yaycılar gabbro – were sent to Actlabs Canada for analysis by Dr. Yakov Kapusta. Geochronologic ages were determined for plagioclase minerals from 5 samples and whole rock sludge for 1 sample with the $^{40}Ar/^{39}Ar$ method. During the sample preparation process, samples were wrapped in aluminium foil for fluid scanning and isotope measurements and bottled in insulated quartz vials. Within the quartz vials, K and Ca salts and LP-6 biotite packets were placed together mixed with samples for fluid monitoring. After studying fluid monitoring, the fluid gradient measured for each sample was used to calculate J values. The age of LP-6 biotite is accepted as 128.1 Ma. In an externally-heated oven, $^{40}Ar/^{39}Ar$ step heating experiments were completed with the temperature value monitored with a thermocouple. Argon isotope analyses were completed with a Micromass 5400 mass spectrometer. Isotope values measured in the mass spectrometer were recorded with the aid of a computer linked to the spectrometer and the process was observed. To check the accuracy of the obtained ages, plateau age calculations were supported by isochron calculations.

4. Sorgun-Yıldızeli Basin Geology

4.1. Stratigraphic, Petrographic and Geochronologic Characteristics

The rock assemblages apparently deposited in two separate E-W oriented basins between Sorgun (Yozgat) and Yıldızeli (Sivas) were determined to be the products of a single large basin (“Sorgun-Yıldızeli basin”) developing due to the same geodynamic processes (Figure 2).

The basin fill is represented mainly by the Boğazköy Formation and its differentiated sub-units. The gabbroic, shallowly emplaced sills and laccoliths into the basal sections of the Boğazköy Formation are distinguished as the Yaycılar gabbro (Figure 3).

4.1.1. Boğazköy Formation

The volcano-sedimentary sequence deposited during the late Palaeocene-middle Eocene period was named as Boğazköy Formation by Özcan et al. (1980) and this is accepted as the formal term by the Turkish Stratigraphy Committee (Turkish Stratigraphy Committee Bulletin (TSKB), 1987).

The section located at the base of Boğazköy Formation and containing slices and olistostromes from IAESZ with generally pelitic, clastic and occasionally poorly sorted coarse clastics are distinguished as the Dolak member.

Toward the interior, and in relatively deeper sections of the basin, three different types of basic, intermediate and acidic composition subduction- and/or collision-related volcanic rocks are interlayered with sparse limestone and with turbiditic conglomerate, sandstone and claystone. These volcanic levels are distinguished as the Pazarcık, Sarayözü and Kiremitlik volcanic members. Reefal limestones in the upper section of the Boğazköy Formation, called the Limestone Member, is generally differentiated from the Konacı member of coarse clastic sediments forming the upper portion of the sequence (Figures 2, 3).

Dolak Member: The Dolak member (Akçay et al., 2008; Dalkılıç et al., 2008) forms the base of the Boğazköy Formation and is generally represented by clastics and coarse-grained clastic rocks. The Dolak member has an olistostromal character in sections close to the thrust line and contains large blocks and slices from the Artova ophiolitic melange and Darmik Formation (Figure 4 a,b,c,d). This unit is equivalent to the Kılıçlı Olistostrome defined in previous studies (Yılmaz, 1982). The Dolak member varies in thickness between 150 and 450 m.

The fossil assemblages identified in the samples from the pelitic levels of Dolak member are given below and according to these fossil assemblages, the late Palaeocene-Lutetian age assigned to the unit: Late Palaeocene-early Eocene: (near Çiçekli village) *Chiasmolithus consuetus* (Bramlette and Sullivan), *Neochiastozygus perfectus* Perch-Nielsen, *Reticulofenestra dictyoda* (Deflandre and Fert),*Coccolithus eopelagicus* (Bramlette and Riedel), *Ericsonia robusta* (Bramlette and Sullivan), *Ericsonia formosa* (Kamptner), *Ericsonia cava (*Hay and Mohler), *Ericsonia ovalis Black*, *Sphenolithus moriformis* (Brönnimann and Stradner), *Toweius tovae Perch-Nielsen*, *Toweius eminens* (Bramlette and Sullivan), *Cruciplacolithus tenius* (Stradner), *Ellipsolithus macellus* (Bramlette and Sullivan), *Fasciculithus tympaniformis* Hay and Mohler nano fossil assemblage.

Late Ypresian-Lutetian: *Ericsonia formosa* (Kamptner), *Discoaster multiradiatus* Bramlette and Riedel, *Toweius eminens* (Bramlette and Sullivan), *Chiasmolithus consuetus* (Bramlette and Sullivan), *Reticulofenestra dictyoda* (Deflandre, Deflandre and Fert), *Zygrhablithus bijugatus* (Deflandre and Fert), *Tribrachiatus bramlettei* (Brönnimann and Stradner), *Ericsonia cava* (Hay and Mohler), *Ericsonia*

Figure 4- Photographs of the Dolak Member which consists of coarse grained clastic sediments (a,b) (west of Kayakışla village) and olistostromal sections (c,d) (northeast of Alicik village).

robusta (Bramlette and Sullivan), *Chiasmolithus consuetus* (Bramlette and Sullivan), *Rhabdosphaera tenius* Bramlette and Sullivan, *Ericsonia formosa* (Kamptner), *Ericsonia obruta* Perch-Nielsen, *Pontosphaera plana* (Bramlette and Sullivan), *Nannotetrina* sp., *Toweius eminens* (Bramlette and Sullivan), *Toweius tovae* Perch-Nielsen, *Sphenolithus primus* Perch-Nielsen, *Coccolithus eopelagicus* (Bramlette and Riedel), *Tribrachiatus orthostylus* Shamrai nano fossil assemblage.

Pazarcık Volcanic Member: This unit described as the Pazarcık Volcanics (Özcan et al., 1980; TSKB, 1987) in previous studies comprises basalt and basaltic andesitic volcanic rocks forming dikes, sills, lava flows and pyroclastic interlayers within the Boğazköy Formation (Figure 5 a,b,c).

The dominant rock type in the Pazarcık volcanic member is basaltic andesite. Basaltic andesite samples have porphyritic and rare amygdoloidal textures. Plagioclase, altered mafic minerals and pyroxene minerals in the form of phenocrystals are distributed in a microlithic texture groundmass. Plagioclase (andesine according to optical properties) minerals display polysynthetic twinning-zoning and sieve texture. Pyroxenes are rarely found and represented by anhedral augite. The iddingsitised mafic minerals are all pseudomorphs and were probably originally olivine. Besides, in some samples, amphibole minerals with partially preserved outer rim and altered to clay and chlorite at the center are found.

Basalts have microcrystalline porphyritic texture, with subhedral-euhedral phenocrysts (mainly

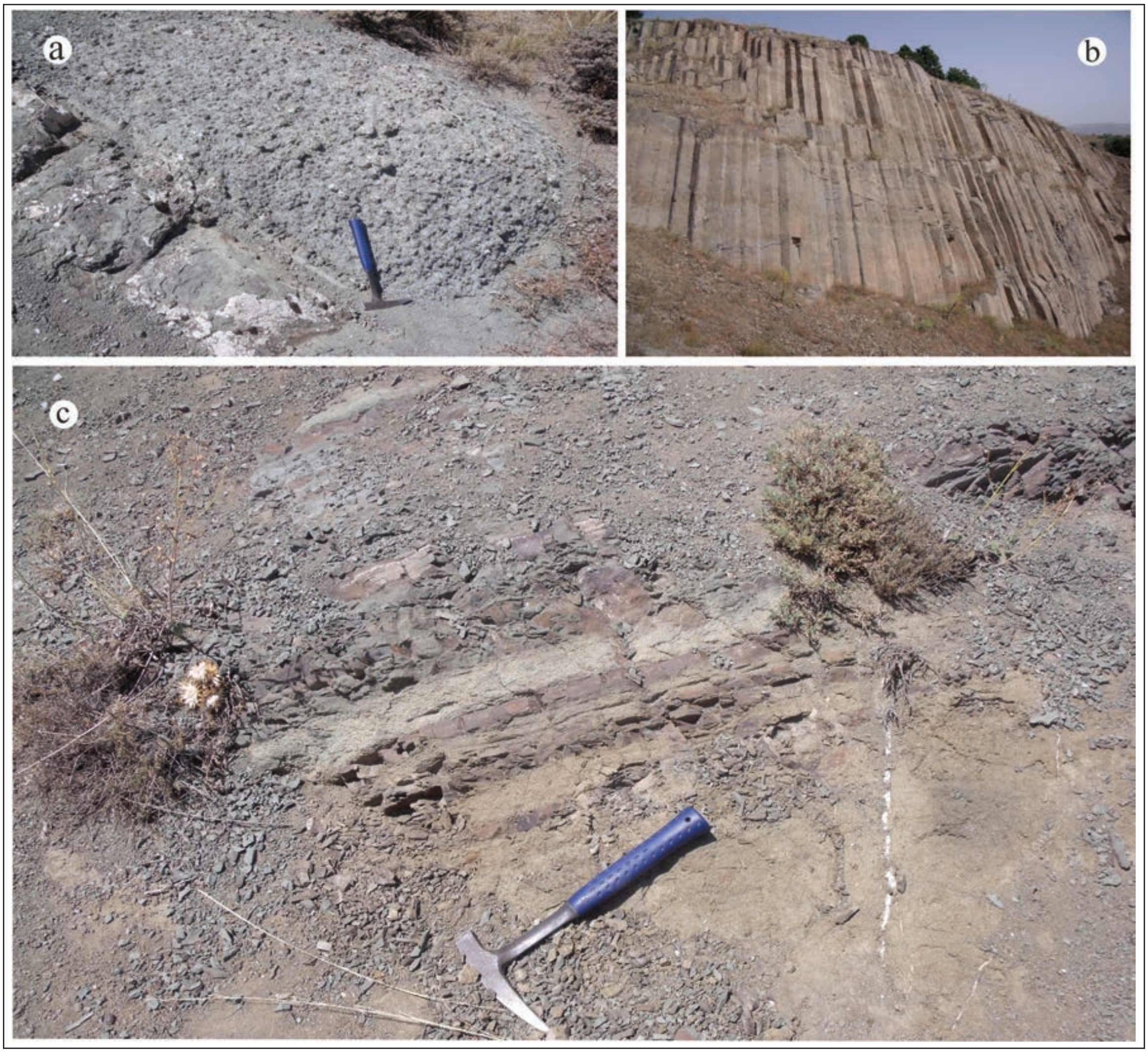

Figure 5- Photographs of the Pazarcık Volcanic Member showing (a) pyroclastic levels (Avcıpnarı village), (b) columnar basalt levels (Pazarcık village) and (c) interlayering within turbiditic sedimentary layers (Avcıpnarı village).

plagioclase, pyroxene, olivine and a few mafic mineral pseudomorphs) in a groundmass of devitrified glass. The majority of plagioclase minerals (andesine-labradorite), comprising the main component, are microlithic, locally forming microphenocrysts, with anhedral and rounded crystal form. Olivines form microphenocrysts which are partially iddingsitised and serpentinized around the rims, with partial or full carbonitisation in the centres. Auxilliary components include opaque minerals with different crystal sizes.

Plagioclase from the Pazarcık volcanic member was dated with the $^{40}Ar/^{39}Ar$ geochronological age methods and yielded age of 57.2±2.0 Ma (Figure 6 a,b), whereas whole rock sludge from a basalt sample from Alimpınar village outside the study area was dated as 56.7±1.8 My (Figure 6 c,d).

Sarayözü Volcanic Member: Dacite, rhyodacite, rhyolitic lava and pyroclastic rocks in the Boğazköy Formation were named as the Sarayözü volcanic member in this study (Figure 7 a,b).

The unit is fragmented by N-S oriented faults and altered near Sarayözü and its northern sections. Hot springs along the valley where the Saray stream flows have locally caused hydrothermal alteration and limonitisation, hematisation and kaolinisation developed in these sections. Locations where limonitisation and hematisation dominate are yellowish-brown or dark brown in colour; whereas in sections where kaolinisation was effective the unit is yellowish-cream and white colour with locally silicification.

In rhyolite samples with porphyritic texture, phenocrysts of quartz, feldspar and rare biotite minerals are distributed within a fine-grained felsic groundmass. The quartz grains are subhedral-anhedral, with partial undulose extinction and grains have experienced magmatic corrosion. Feldspars are euhedral comprising albite-oligoclase composition plagioclases. In samples, quartz and feldspars rarely form glomeroporphyric texture. Samples with spherulitic textures are found within rhyolitic lava.

Plagioclase in dacite from the Sarayözü volcanic member yielded $^{40}Ar/^{39}Ar$ age of 48.8±1.5 Ma (Figure 8 a,b).

Kiremitlik Volcanic Member: This unit is composed dominantly of andesitic lava and pyroclastic rocks.

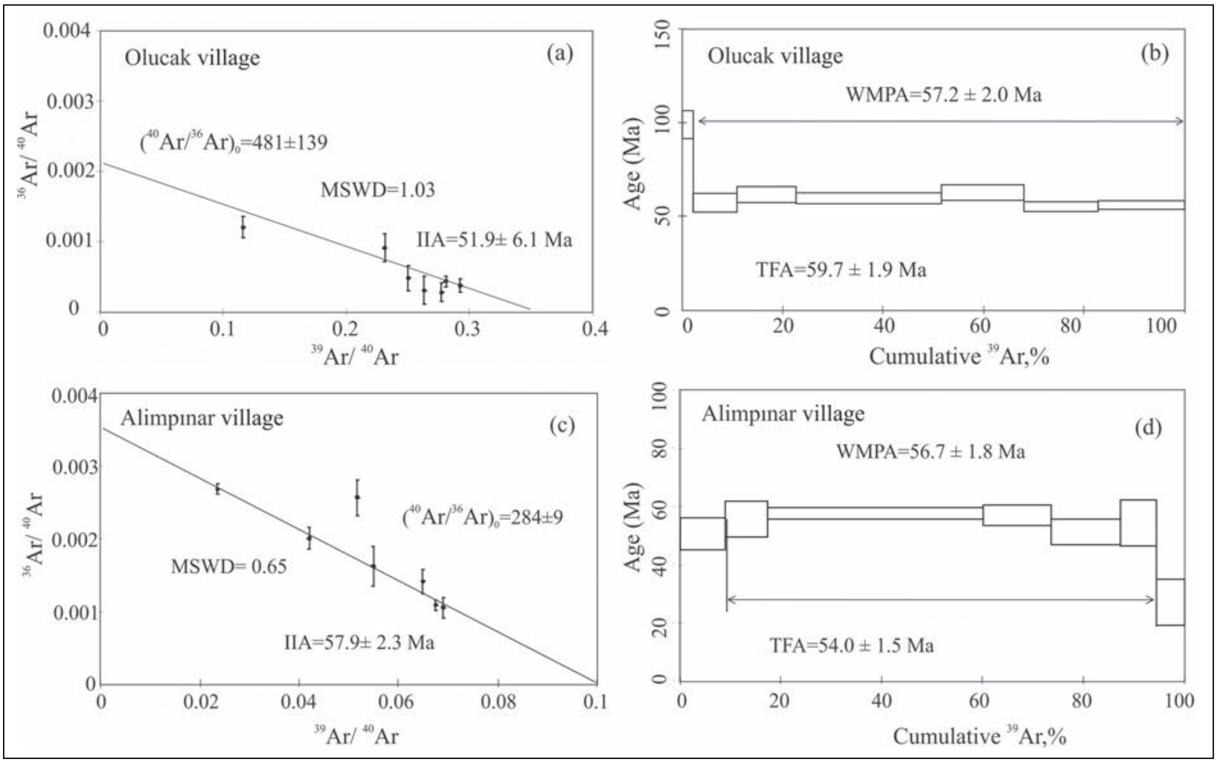

Figure 6- Age dates of two basalt samples from the Pazarcık volcanic member; plagioclase (a, b) and whole rock (c, d) isochron and plateau age diagrams (IIA = inverse isochron age; TFA= total fission age; WMPA= weighted mean plateau age; MSWD: mean square weighted deviation).

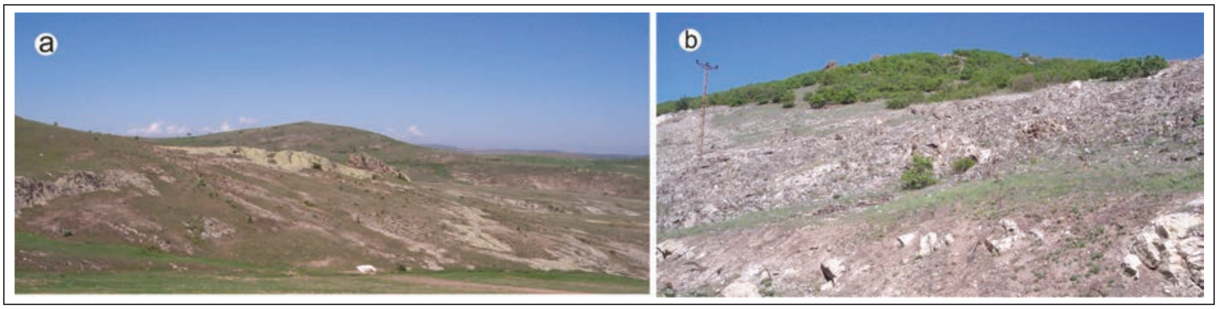

Figure 7- Photographs showing the Sarayözü volcanic member; a view from rhyolite dome(a) and rhyolite with advanced degree of alteration (b) (Sarayözü village).

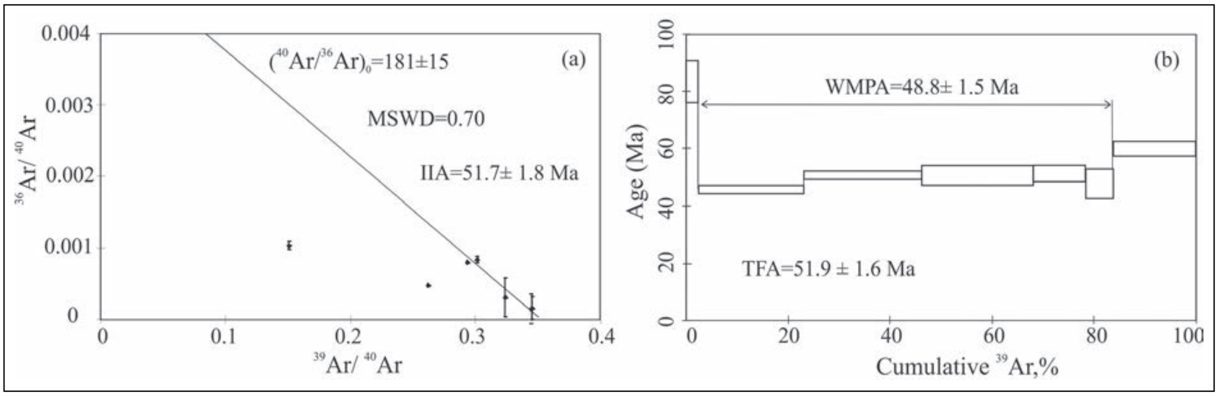

Figure 8- Radiometric age dates on plagioclase from dacites in the Sarayözü volcanic member showing isochron (a) and plateau age (b) diagrams (Gökdere village-Çarşak Tepe).

It is located in the upper sections of the Boğazköy Formation and was named as the Kiremitlik volcanic member in this study (Figure 9).

The unit has been defined as andesite, hyaloandesite and pyroxene andesite by petrographic investigations. Andesites have porphyritic texture with phenocrysts of plagioclase, mica and rare amphibole in a microlithic groundmass. Plagioclase is mainly represented by polysynthetic twinned-zoned oligoclase-andesine types. In some samples, plagioclase is intensely carbonitised, partially argillised and the grains

Figure 9- Photographs showing the andesites terrains of the Kiremitlik volcanic member (south of Kiremitlik Tepe).

locally combine to form glomeroporphyric texture. Amphiboles have opacity and occasionally the interior is in the form of chloritised pseudomorphs. Micas are fine to coarse grained, partially euhedral with partial opacity of prismatic forms and biotite minerals display opaque mineral exsolutions. Altered mafic minerals with preserved outer rims are possibly amphibole minerals in the form of chlorite-carbonate pseudomorphs. Mafic minerals rarely have opacity. Flow textures observed in the groundmass consist of plagioclase microliths in a glassy matrix. Samples with more volcanic glass in groundmass are described as hyaloandesite.

Pyroxene andesite has similar mineral paragenesis as does the hyaloandesites; however it is distinguished by containing a much lower amount of volcanic glass material. Pyroxene andesite has porphyritic texture. Phenocrysts of plagioclase, pyroxene and altered mafic minerals are distributed in a groundmass with microgranular texture. Plagioclase is partially chloritised-sericitised with polysynthetic twinning-zoning and an oligoclase-andesine character. Pyroxene is fine to coarse grained and partially euhedral augite. Altered mafic minerals are chloritised and carbonitised amphibole minerals. In addition, mafic mineral relicts from which iron oxide is completely removed were identified. Feldspar and pyroxene minerals rarely occur together to form a glomeroporphyric texture.

Plagioclase in andesite from the Kiremitlik volcanic member yielded $^{40}Ar/^{39}Ar$ geochronologic ages of 45.1±1.3 and 47.3±0.6 Ma (Figure 10 a,b,c,d).

Limestone Member: Levels of clastic-clayey limestone and limestone in the upper sections of the Boğazköy Formation were named as the Limestone member (Akçay et al., 2008; Dalkılıç et al., 2008). The unit represents neritic limestone with yellowish-grey, yellowish-cream, locally beige colour, thick to very thick bedded and generally fossiliferous limestone. The maximum thickness measured is 34 m. The unit was formed in a calm shallow marine environment. Samples obtained from different levels of the Limestone member of the Boğazköy Formation contain *Assilina* gr. *exponens* Sowerby, *Nummulites* sp., *Asterigerina* sp., *Discocyclina* sp., *Lockhartia* sp., *Acarinina* sp., *Globigerina* sp., *Morozovella*

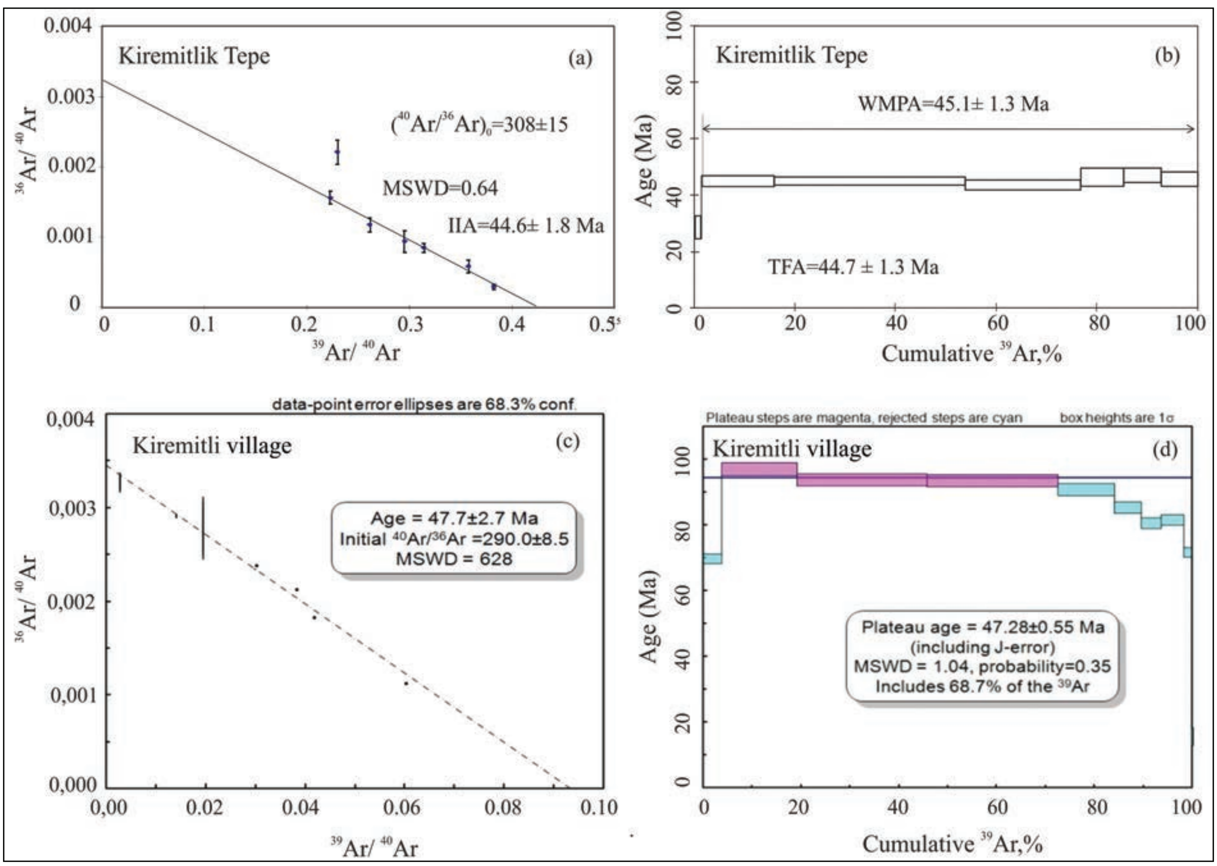

Figure 10- Plagioclase isochron and plateau age diagrams from two andesite samples belonging to the Kiremitlik volcanic member (Kiremitlik Tepe and Kiremitli village).

sp., Miliolidae, Rotaliidae, Textulariidae algae, bryozoans and macro shell fragments. According to this palaeontological data, it is dated to the Lutetian.

Konacı Member: The uppermost levels of the Boğazköy Formation, generally represented by clastic rocks, are named as the Konacı member (Özcan et al., 1980). The unit contains siltstone, sandstone and conglomerate with claystone and clayey limestone interlayers (Figure 11). The dominant rock type is observed to be intercalations of conglomerate and sandstone. The conglomerate is greyish yellow, yellow and pale colours, massive, medium to thick layered with locally thin layers. Clasts vary from very small to very large in size and are subangular to rounded, matrix-supported, and locally well sorted and polygenic. The unit does not show lateral continuity, but has apparent thickness of nearly 300 m.

Samples obtained from clayey limestone levels in the Konacı member which form the uppermost levels of the Boğazköy Formation include *Acarinina spinuloinflata* (Bandy), *Acarinina bullbrooki* (Bolli), *Acarinina* cf. *pentacamerata* (Subbotina), *Turborotalia frontosa* (Subbotina), *Turborotalia* sp., and *Morozovella* sp. with an early-middle Eocene (late Ypresian-Lutetian) age. However, when the stratigraphic location of the member and the middle Eocene radiometric age for the underlying volcanic rocks are considered together, Konacı member is assigned to the middle Eocene.

4.1.2. Yaycılar Gabbro

Gabbroic rocks emplaced as sills and laccoliths in the basal sections of the Boğazköy Formation are named the Yaycılar gabbro (Figure 12 a,b).

The Yaycılar gabbro mainly consists of plagioclase and pyroxene with lesser biotite and opaque minerals. The majority of the pyroxene group minerals are anhedral clinopyroxenes, accompanied by a small amount of orthopyroxene. Plagioclase is the other significant component and is characterised by twinning and prismatic shape. The Yaycılar gabbro generally displays granular texture. Ophitic texture can also be observed in some samples.

The Yaycılar gabbro is cut by a micro-monzonite dike-vein systems with a thickness ranging between 5-10 cm (Figure 12 a). Veins cutting the gabbro have holocrystalline granular texture and monzonitic composition. They contain potassium-feldspar, plagioclase and secondary calcite minerals. The majority of the feldspars are argillised. Chloritisation is observed within the rocks and opaque minerals are common. At the boundary zone between the monzonitic dike-vein systems and gabbro, the gabbro displays an advanced degree of alteration and weathering.

Plagioclase from the Yaycılar gabbro yielded $^{40}Ar/^{39}Ar$ geochronologic age of 51.0±0.7 Ma (Figure 13 a,b).

Figure 11- Photographs showing the general appearence of clastic rocks forming the Konacı member (Konacı village).

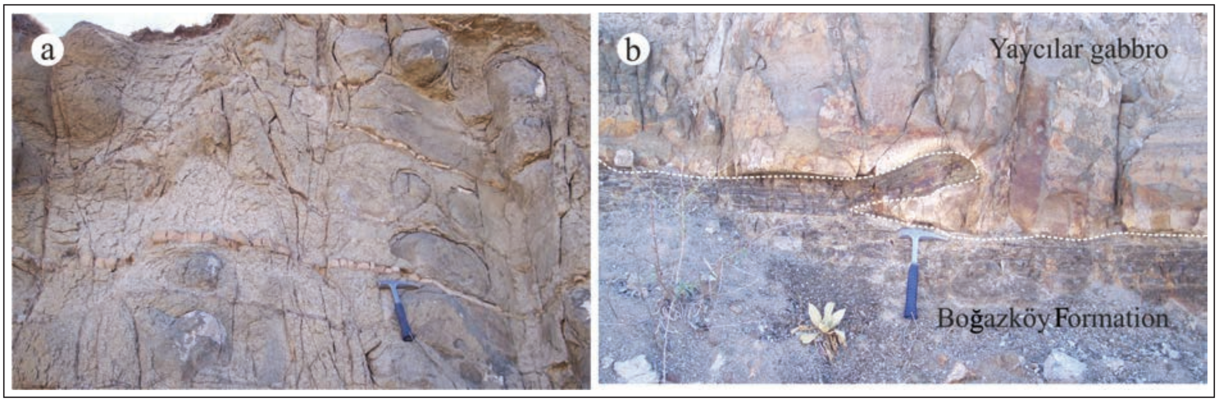

Figure 12- Photographs showing the Yaycılar gabbro; dike-vein systems with micro-monzonitic composition (a) and intrusive contact of the gabbro with the Boğazköy Formation (b) (Karakız village).

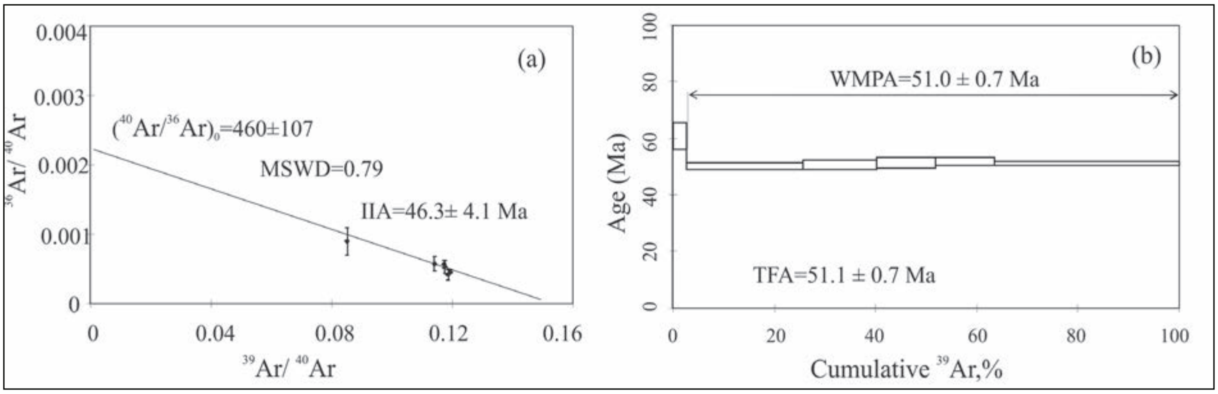

Figure 13- Plagioclase isochron (a) and plateau (b) age diagrams from Yaycılar gabbro (Yaycılar village).

4.2. Geochemical Characteristics

To characterise the volcanism affecting the Sorgun-Yıldızeli foreland basin geochemically, a total of 17 samples were collected from members of the Boğazköy Formation including 5 samples from the basaltic Pazarcık volcanic member, 6 samples from the andesite-dacite Kiremitlik volcanic member and 6 samples from the Yaycılar gabbroic sills and laccoliths in the basal sections of the Boğazköy Formation. As the Sarayözü member had undergone an advanced degree of alteration, fresh samples appropriate for analysis could not be obtained. The results of the chemical analyses are given in table 1.

4.2.1. Classification

The Pazarcık and Kiremitlik volcanic members and the Yaycılar gabbro were classified on the total alkali versus silica (TAS) diagram (Le Bas et al. 1986) (Figure 14 a) and the Pazarcık volcanics generally have basaltic composition. Samples mainly plot in the basaltic andesite, trachybasalt and basaltic trachyandesite fields. One of the samples from the Kiremitlik volcanic member is trachyandesite and another is rhyolite, the rest are s dacite in composition.

As seen in table 1, some of the samples has very high loss on ignition values (LOI), ranging between 3.95-9.06 in the Pazarcık volcanic member, 0.80-3.68 in the Kiremitlik volcanic member and 3.09-4.53 in the Yaycılar gabbro. In petrographic investigations, some of the samples from Kiremitlik member have thin to thick carbonate and silica veinlets and filling cavities and iron oxide on fractures, indicating the role of alteration processes which also affect the chemical results.

As hydrothermal alteration processes may cause changes in the major oxide values of rocks (especially SiO_2, CaO, K_2O and Na_2O), the samples are plotted on the SiO_2-Zr/TiO_2 diagram of Winchester and Floyd (1977) and the Zr/Ti-Nb/Y diagram modified by Pearce (1996), utilising less mobile elements to classify altered rocks. due tolow alteration and metamorphism conditions (Figure 14 c,d). In figure

Table 1- Whole rock (major, trace and rare earth elements) chemical analysis results for rock samples from the Pazarcık volcanic member, Kiremitlik volcanic member and Yaycılar gabbro.

SAMPLE NO	KİREMİTLİK VOLCANIC MEMBER						PAZARCIK VOLCANIC MEMBER					YAYCILAR GABBRO					
	K1	K2	K3	K4	K5	K6	P1	P2	P3	P4	P5	G1	G2	G3	G4	G5	G6
Major Oxides Wt.%																	
SiO_2	59	62,2	65,7	67,6	68,9	66	49,9	49	48,7	48,3	49,3	46,8	50,5	48,9	47,9	49,3	50,6
Al_2O_3	16,7	15,75	16,8	15,55	15,4	15,5	15,3	16,35	16,5	15,95	16,3	16,05	17,4	16,9	16,85	16,9	19
Fe_2O_3	6,08	5,11	2,77	3,84	2,85	3,47	9,85	9,92	10,45	9	10,1	11,65	10,45	10,65	11,25	10,7	8,5
CaO	3,72	4,43	3,78	3,74	3	3,84	8,46	8,68	7,97	10,05	9,08	8,7	8,08	8,06	9,24	8,84	7,75
MgO	1,84	0,44	0,33	0,6	0,49	0,5	5,42	4,64	5,01	3,18	4,76	5,93	4,02	4,95	5,4	4,17	4,29
Na_2O	5,37	3,91	4,42	4,09	4,51	4,28	4,55	3,42	4,41	2,96	3,47	3,81	4,06	3,84	3,25	4,02	4,36
K2O	2,14	2,72	2,7	2,63	3,18	2,86	1,67	1,56	2,04	1,1	2,07	1,44	2,1	1,65	1,39	1,6	1,98
Cr_2O_3	<0.01	<0.01	<0.01	0,01	<0.01	<0.01	0,01	<0.01	<0.01	<0.01	<0.01	0,01	<0.01	<0.01	0,01	<0.01	0,01
TiO_2	0,66	0,69	0,67	0,59	0,47	0,58	0,94	1,01	1,14	0,97	1,05	1,15	1,22	1,12	1,15	1,14	0,9
MnO	0,08	0,06	0,01	0,03	0,04	0,03	0,18	0,17	0,18	0,15	0,17	0,19	0,17	0,18	0,17	0,17	0,08
P_2O_5	0,31	0,27	0,27	0,22	0,17	0,24	0,28	0,25	0,29	0,25	0,34	0,24	0,31	0,28	0,24	0,26	0,24
SrO	0,03	0,05	0,05	0,04	0,04	0,05	0,06	0,06	0,07	0,05	0,08	0,08	0,07	0,07	0,06	0,05	0,09
BaO	0,06	0,1	0,1	0,13	0,1	0,12	0,06	0,06	0,06	0,04	0,06	0,06	0,05	0,04	0,04	0,05	0,05
Loss on Ignition	3,68	2,84	2,8	2,16	0,8	1,54	4,86	6,15	5,03	9,06	3,95	4,53	3,19	4,3	3,26	4,23	3,81
Total	99,67	98,57	100,4	101,23	99,95	99,01	101,54	101,27	101,85	101,06	100,73	100,64	101,62	100,94	100,21	101,43	101,66
Trace Elements ppm																	
Ba	492	777	811	1005	805	933	535	467	488	339	513	469	385	349	364	375	370
Cr	10	30	20	40	20	20	50	10	20	10	20	50	20	40	40	30	60
Cs	1,13	2,75	1,91	2,1	2,43	2,15	3,32	1,03	6,02	0,66	1,29	1,8	0,67	0,71	0,66	2,5	1,25
Ga	19	17,7	19,1	17,1	16,8	17,2	18	18,7	18,7	18,3	18,6	18,7	19,6	19,3	18,7	19,6	18,8
Hf	4,4	4,4	5	4,6	4,9	4,6	2,8	2,9	2,7	2,7	3,1	2,1	2,7	2,6	2,2	3	2,3
Nb	9,3	11,1	13,3	10,5	12,5	11,8	6,5	4,8	5,2	6,2	7,8	3,6	5,4	4,7	3,8	5,3	4,7
Rb	56,2	81,7	58,1	82,1	108	91,9	46,6	32,1	45,9	24,1	61	28,1	50,8	31,8	32,1	33,9	49,1
Sn	1	1	1	1	1	1	1	1	1	1	1	1	1	1	1	1	1
Sr	336	463	497	431	388	468	491	550	571	501	710	713	614	626	574	447	762
Ta	0,6	0,8	1	0,8	1	0,9	0,3	0,2	0,3	0,3	0,4	0,1	0,3	0,2	0,2	0,3	0,2
Th	7,19	15,55	18,65	15,05	20	18	5,29	7,06	4,21	5,38	5,9	5,8	3,8	3,7	3,03	4,46	3,23
Tl	<0.5	<0.5	<0.5	<0.5	<0.5	<0.5	<0.5	<0.5	<0.5	<0.5	<0.5	<0.5	<0.5	<0.5	<0.5	<0.5	<0.5
U	1,65	3,24	2,39	3,2	4,45	4,13	1,43	2,24	1,19	1,1	1,55	1,22	0,92	0,87	0,72	1,08	0,8
V	98	101	107	102	79	98	280	267	300	249	277	385	295	290	375	287	225
W	<1	1	1	<1	1	1	<1	<1	<1	<1	<1	<1	<1	<1	<1	<1	<1
Y	27	20	18,8	18,7	15,8	17,6	24,3	23,4	24,9	22,3	25,1	22,7	26,2	25,5	21,8	26,7	19,9
Zr	159	156	181	160	172	168	93	91	87	87	99	62	86	83	68	98	75
As	0,8	2	1,3	1,7	1,3	0,9	0,6	3,5	0,2	0,2	1,1	0,3	<0.2	1,7	0,8	1,2	<0.2
Be	1,55	1,31	1,4	1,58	1,6	1,76	1,27	1,04	1,11	0,88	1,37	0,88	1,05	0,9	0,8	1,22	1,02
Bi	<0.01	0,1	0,07	0,04	0,06	0,04	0,02	0,17	0,04	0,03	0,07	0,04	0,02	0,07	0,04	0,05	0,02
Cd	0,05	0,06	0,02	0,02	0,02	0,03	0,11	0,08	0,16	0,08	0,1	0,1	0,09	0,15	0,12	0,07	0,04
Co	10,8	7,5	3,8	5	3,1	5,6	30,2	28,6	32,6	26,7	32,2	37,8	30	32,9	37,4	34,2	26,5
Cu	11,8	15,5	17,4	20,6	8,2	45,6	111,5	49,2	96,4	28,4	109	105	113	142,5	89,3	102	14,6
Ge	0,2	0,12	0,12	0,13	0,14	0,16	0,17	0,11	0,12	0,11	0,11	0,1	0,11	0,1	0,08	0,1	0,08
Mo	0,84	0,62	0,66	1,09	1,52	1,27	0,76	0,82	0,86	0,41	1,1	0,74	1,05	0,92	0,5	0,81	1,06
Ni	2,4	8,3	4,6	11,3	5,7	8,3	26,3	9,9	20	10,4	23,5	32,5	16,3	23,3	25	23,5	23,5
Pb	8,3	15,9	17,3	14,1	18,2	16	10	13,2	4,9	5,8	8,8	6,6	4,5	3,3	3,6	3,9	1,8
Sb	0,23	0,36	0,37	0,26	0,41	0,26	0,16	0,52	0,15	0,18	0,21	0,1	0,11	0,15	0,15	0,21	0,1
Zn	45	24	37	36	29	15	89	78	86	71	77	89	74	75	70	82	28
Rare Earth Elements ppm																	
Ce	45,6	58,5	68,8	59,5	61	73,5	37,4	37,3	34,2	41,1	42,3	36,8	31	30,4	24,5	33,2	25,6
Dy	4,52	3,55	3,4	3,24	2,77	3,09	4,44	4,28	4,47	4,03	4,51	4,17	4,71	4,47	3,97	4,71	3,58
Er	2,88	2	2,08	2,02	1,68	1,89	2,52	2,63	2,63	2,43	2,55	2,39	2,8	2,75	2,3	2,92	2,16
Eu	1,34	1,18	1,26	1,1	0,97	1,15	1,37	1,41	1,4	1,33	1,38	1,41	1,41	1,35	1,19	1,37	1
Gd	4,75	3,88	4	3,8	3,21	3,75	4,84	4,62	4,88	4,25	5,06	4,66	4,85	4,83	3,97	4,84	3,59
Ho	1,03	0,77	0,73	0,72	0,6	0,69	0,94	0,94	0,97	0,88	0,97	0,91	1,06	0,98	0,86	1,07	0,77
La	25	33,7	38,9	33,4	36,5	42,6	19	19,1	16,7	20,6	21,3	19,1	15,3	14,8	12	16,5	12,8
Lu	0,47	0,34	0,36	0,32	0,29	0,32	0,37	0,38	0,39	0,34	0,39	0,34	0,42	0,41	0,35	0,44	0,34
Nd	21,8	23,1	26,3	23,2	20,9	27,1	19,4	19,3	19,2	20	21,7	19,7	17,7	17,4	14,3	18,3	13,7
Pr	5,78	6,57	7,66	6,83	6,57	8,11	4,83	4,82	4,51	5,21	5,48	4,79	4,14	4,15	3,4	4,38	3,37
Sm	4,47	4,28	4,51	4,05	3,4	4,37	4,24	4,38	4,45	4,18	4,87	4,36	4,26	4,12	3,55	4,42	3,15
Tb	0,74	0,58	0,62	0,59	0,48	0,55	0,72	0,72	0,74	0,66	0,74	0,7	0,77	0,75	0,65	0,79	0,57
Tm	0,43	0,31	0,31	0,29	0,25	0,28	0,36	0,37	0,36	0,33	0,37	0,34	0,41	0,39	0,34	0,43	0,3
Yb	2,88	2,15	2,17	1,92	1,71	1,97	2,29	2,39	2,49	2,25	2,49	2,17	2,63	2,51	2,21	2,76	2,1
Mg#	37,50	14,60	19,10	23,60	25,40	22,20	52,20	48,10	48,70	41,20	48,30	50,20	43,30	47,90	48,70	43,60	50,00
Eu/Eu*	0,89	0,89	0,91	0,86	0,90	0,87	0,93	0,96	0,92	0,97	0,85	0,96	0,95	0,93	0,97	0,91	0,91

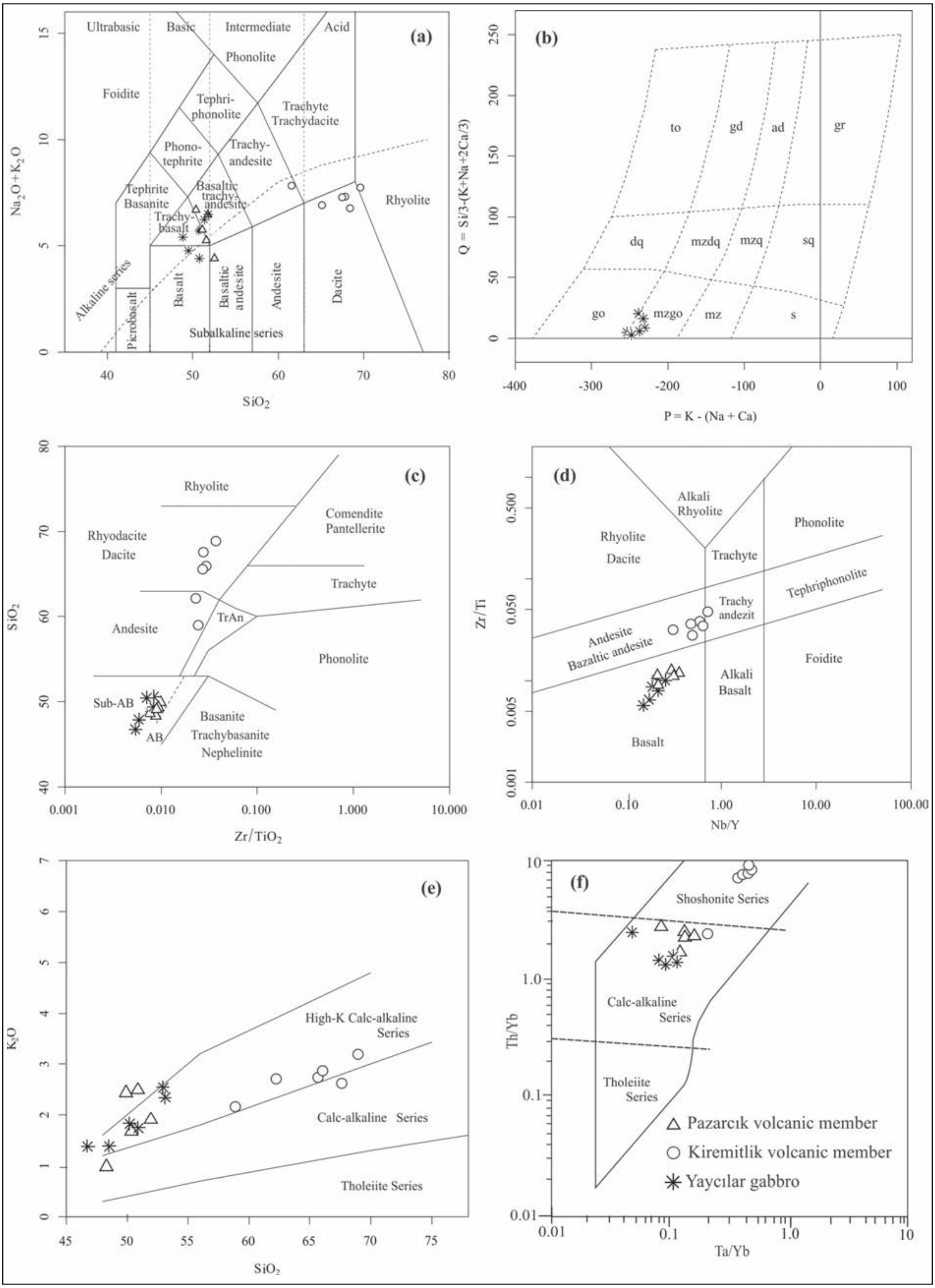

Figure 14- Classification diagrams of Pazarcık and Kiremitlik volcanic rocks (a) Le Bas et al. (1986), (b) Debon and Le Fort (1983), (c) Winchester and Floyd (1977), (d) Pearce (1996), (e) Peccerillo and Taylor (1976), and (f) Pearce (1983).

14c, d, samples from the Pazarcık volcanic member and the Yaycılar gabbro exhibit sub-alkaline trend and are basalt in composition. Two samples from the Kiremitlik volcanic members are andesite and four samples are rhyodacite/dacite in composition (Figure 14 c). On Pearce's (1996) Zr/Ti-Nb/Y diagram, samples from the Pazarcık volcanic member and the Yaycılar gabbro plot in the field of basalt, samples from the Kiremitlik volcanic member range in composition from andesite/basaltic andesite to trachyandesite (Figure 14 d). It is apparent from the classification diagrams that samples of the Kiremitlik volcanic member have partially experiencedalteration (silicification). Thus, the most plausible classification diagram for altered samples is the Zr/Ti-Nb/Y diagram of Winchester and Floyd (1977) modified by Pearce (1996). Consequently, based on petrographic data and Zr/Ti-Nb/Y classification diagram, the Pazarcık and Kiremitlik volcanic member are the products of basaltic and andesitic volcanism, respectively.

Samples from the Yaycılar gabbro is similar to that of the Pazarcık volcanic member on the TAS diagram, but on the P-Q diagram of Debon and Le Fort (1983) they are classified as gabbro-monzogabbro (Figure 14 b).

Samples are plotted on the SiO_2 versus K_2O diagram of Peccerillo and Taylor (1976) and Ta/Yb-Th/Yb diagram of Pearce (1983) utilising less-mobile elements (such as Th, Ta and Yb) during alteration (Figure 14 e,f). It is clear from the figure 14e that they generally exhibit calcalkaline trend (or high-K calcalkaline), except 2 samples from the Pazarcık volcanic having shoshonitic affinities (Figure 14 e). On the Ta/Yb versus Ta/Yb diagram (Pearce, 1983), samples from the Pazarcık volcanic member and Yaycılar gabbro have calc-alkaline trends, the great majority of the samples from the Kiremitlik volcanic member are clearly plotted in the field of shoshonite (Figure 14 f).

Samples from the Kiremitlik volcanic member have geochemical features similar to shoshonites with their low TiO_2 and Fe_2O_3 contents, enrichment in Ba, Rb, Ce and Pb elements and high total alkali (Na_2O + K_2O > 5%) contents, despite having low K_2O values relative to Na_2O (K_2O / Na_2O <1)

According to Morrison (1980), in subduction belts during consumption of the subduction phase shoshonitic rocks may be formed related to arc deformation.

Though the magma source generating the Kiremitlik volcanic member may not be typical, the similar characteristics to shoshonitic magma may be due to hot asthenospheric mantle rising during slab breakoff and pushed deep under the continent by subduction and collision events causing crustal material to melt or due to crustal contamination during ascent of magma through continental crust.

4.2.2. Major Oxides and Trace Element Characteristics

In order to determine the role of fractional crystallisation processes, variation diagrams of major-oxides are plotted against SiO_2 in figure 15. It is clear from the figure there is a negative correlation between SiO_2 and CaO, MgO, TiO_2, and FeO_t, a positive correlation between SiO_2 and Na_2O, K_2O. The plots of SiO_2 against Al_2O_3, P_2O_5 in Pazarcık volcanic member and Yaycılar gabbro exhibit roughly vertical trends with increasing Al_2O_3 and P_2O_5, but in Kiremitlik volcanic member, there is a clear negative correlation between SiO_2 and Al_2O_3, P_2O_5.

The negative correlations between SiO_2 and FeOt, MgO, CaO, TiO_2 are qualitatively related with the removal of olivine, pyroxene, Ca-plagioclase and titanohematites from the melt at the beginning of crystallisation. The positive correlation between SiO_2 and K_2O, Na_2O may also indicate a fractionation trend, since Na-plagioclase and mica minerals are the last minerals to crystallise from a melt and thus, they become enriched within a melt during fractional crystallisation.

The variation diagrams of SiO_2 versus trace elements (Rb, Ba, Sr, Zr, Nb, Sm, Ni, Co, Th, La, Y, V) are given in figure 16. On these diagrams, there is a positive correlation between SiO_2 and Rb, Ba, Th, Zr, Hf, Nb, and La elements. These elements occur within minerals forming during slightly later stages of crystallisation and thus show positive correlation. Sr, Sm, Ni, Co, Y, and V elements occur within minerals crystallising in the early stages so they show negative correlation with SiO_2. The positive correlation between SiO_2 and Rb, Ba and Th elements can be explained by fractionation of feldspars and amphiboles, the negative trend of Sr is due to substitution of Sr for Ca in Ca-plagioclase and removal of Ca-plagioclase from the melt at the early stages of fractional crystallisation.

The magnesium number (Mg# = molar 100xMgO/[MgO+tFe_2O_3]) of the Pazarcık volcanic member

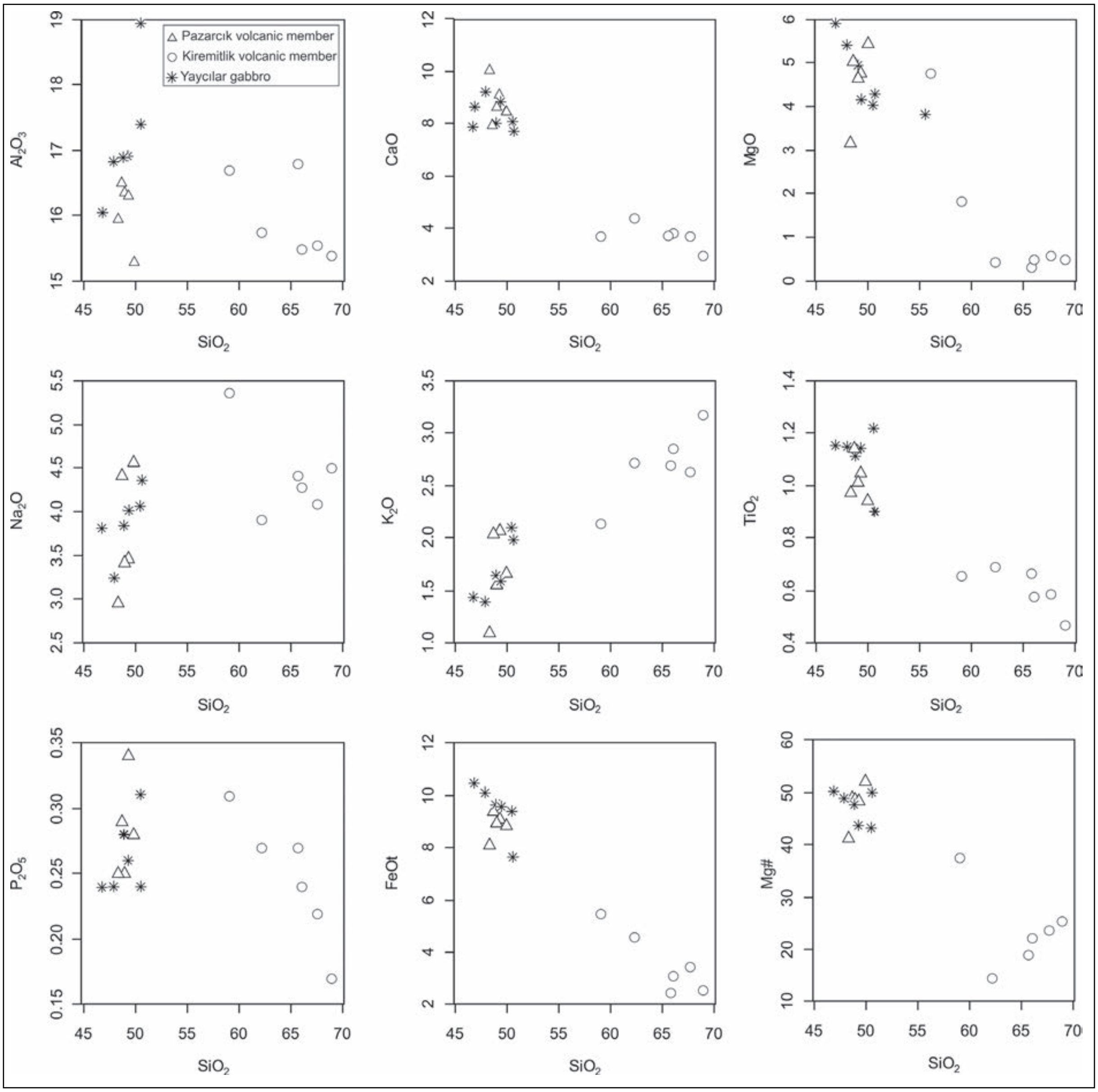

Figure 15- SiO_2 (%) versus major oxide (%) variation diagrams for Pazarcık and Kiremitlik volcanic members and Yaycılar gabbro.

ranges from 41.18 to 51.26, from 43.25 to 50.21 in the Yaycılar gabbro and from 14.37 to 37.48 in the Kiremitlik volcanic member.

The observed variations on Harker diagrams and the moderate-low Mg number of the units indicate that they have experienced variable amounts of fractional crystallisation and as a result, the volcanism in the Sorgun-Yıldızeli basin was derived from evolved magma.

The variation diagrams of SiO_2 versus major oxides and trace elements display that samples from the Pazarcık and Kiremitlik volcanics form separate groups, with fractional crystallisation trends within each group. This may be due to different reasons such as crustal contamination, residence time within the crust, variable degree of partial melting of the magma source, evolution of the magma as a result of a single fractional crystallisation process, or developments of magmatic processes in separate stages.

4.2.3. Trace and Rare Earth Element (REE) Characteristics

Mid-Ocean Ridge Basalts (MORB) and chondrite-normalised multi-element distribution diagrams of

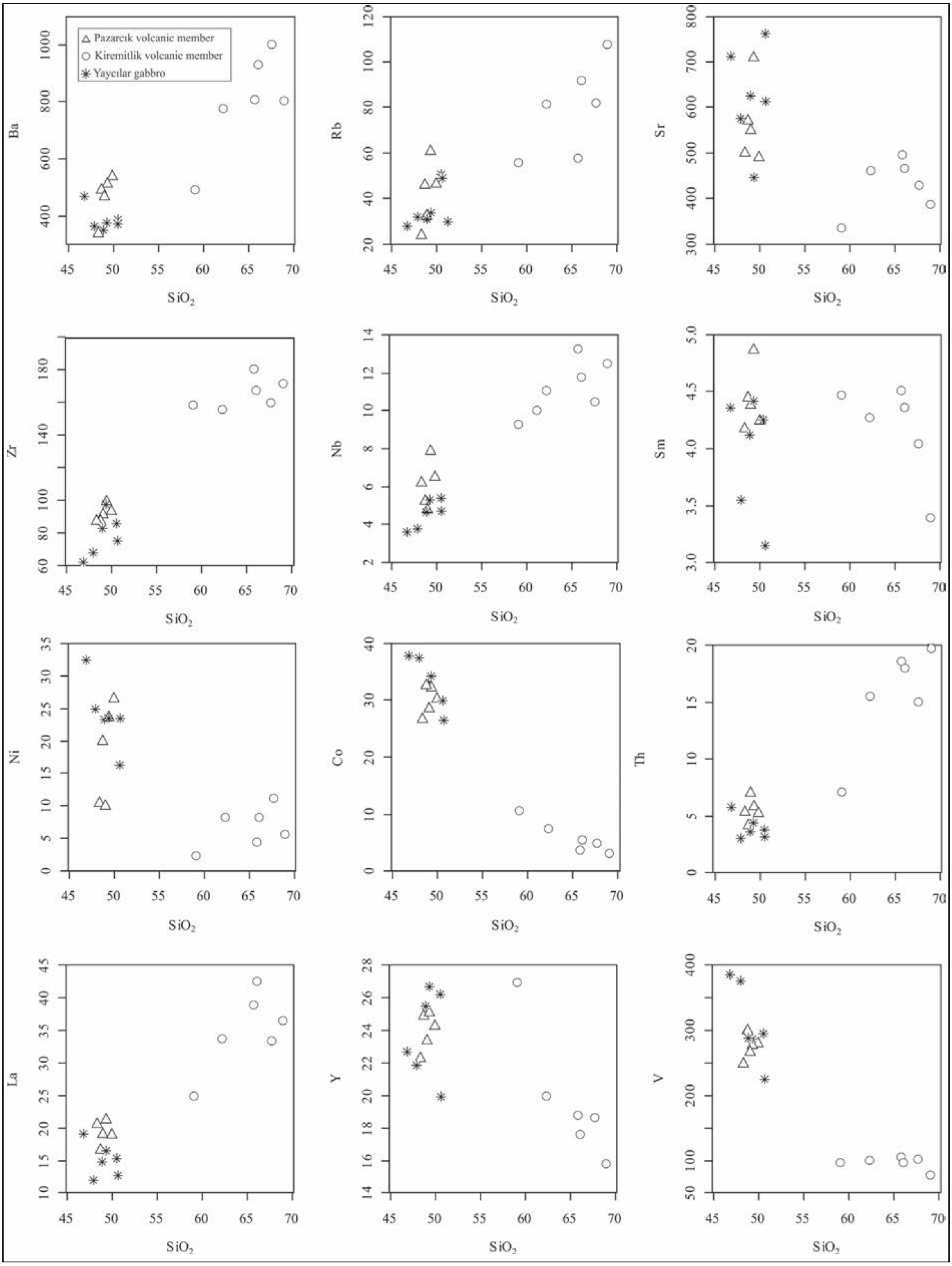

Figure 16- SiO_2 (%) versus trace element (ppm) variation diagrams for Pazarcık and Kiremitlik volcanic members and Yaycılar gabbro.

Pazarcık and Kiremitlik volcanic samples are illustrated in figure 17 to determine the source characteristics of the volcanic rocks. Features common for all samples are the enrichment in large ion lithophile elements (Sr, K, Rb, Ba and Th) and the depletion in Nb, Ta, Ti, Y and Yb elements. Clear enrichment in large ion lithophile elements combined with the Nb-Ta negative anomaly are similar to characteristic geochemical properties of active continental margin or arc magmatism and indicate the presence of subduction components in magma source (Gill, 1981; Fitton et al., 1988; Pearce, 1983; Wilson, 1989). Depletion of Y and Yb elements is considered to be due to the presence of amphibole and/or some garnet (Figure 17 a).

On chondrite - normalised multi - element distribution diagrams, light rare earth elements (LREE) appear to be enriched relative to heavy rare earth elements (HREE). The concave distribution of rare earth elements may correspond to the fractional crystallisation process and the removal of amphibole and pyroxene minerals during fractionation (Figure 17 b).

The Eu/Eu* ratios ($Eu/Eu^* = Eu_n/(Sm_n + Gd_n)^{0.5}$) are 0.85-0.97 for the Pazarcık volcanic member, 0.9-0.97 for the Yaycılar gabbro and 0.86-0.91 for the Kiremitlik volcanic member. If this ratio is larger than 1, a positive anomaly is present, if it is smaller than 1, a negative anomaly exists. According to these values, the Yaycılar gabbro has a weak negative Eu anomaly, while the Pazarcık and Kiremitlik volcanic member have a moderate degree of negative anomaly. This negative anomaly indicates fractional crystallisation and plagioclase fractionation.

4.2.4. Effects of Subduction Components and/or Crustal Contamination

With the aim of determining whether subduction zone enrichment and/or crustal contamination with intraplate enrichment was effective on the genesis of the Yaycılar gabbro and Pazarcık and Kiremitlik volcanics, samples are assessed on diagrams using trace element ratios such as Th/Y, Nb/Y and Rb/Y (Figure 18 a,b).

The Th/Nb ratio of samples from the Yaycılar gabbro is 0.70-1.61, while this ratio is 0.76-1.47 for Pazarcık volcanic samples and 0.77-1.60 for samples from the Kiremitlik volcanic member. When the Th/Y against Nb/Y diagram is examined, samples appear to plot close to the Th/Nb=1 line. Th is enriched in continental crust, while Nb is found at smaller amounts. High Th/Nb ratios indicate that rocks have experienced crustal contamination (Pearce, 1983). This contamination may be due to subduction effects, but may also be due to assimilation of wall rocks during the rising of magma to the surface. With the increase in Nb/Y ratio, increasing Th/Y shows intraplate enrichment, while low Nb/Y ratios with increasing Th/Y ratio shows subduction zone enrichment (Figure 18 a).

On the Rb/Y-Nb/Y diagram, Rb/Nb=1 line indicates intraplate enrichment, while vertical trend shows subduction zone enrichment and/or crustal contamination (Edwards et al., 1991). The Rb/Nb ratios vary from 6.40 to 10.45 in samples from the Yaycılar gabbro, 3.89-8.83 in the Pazarcık volcanic member and 4.37-8.64 in the Kiremitlik volcanic member. The vertical trend shows that subduction zone enrichment and/or crustal contamination has played a significant role in the evolution of magma. The magma generating the Kiremitlik volcanic member experienced greater crustal contamination and/or intraplate enrichment relative to the Pazarcık volcanic member (Figure 18b).

4.2.5. Tectonic Environment

The Pazarcık and Kiremitlik volcanic members and Yaycılar gabbro were evaluated on tectonic discrimination diagrams (Figure 19 a,b,c,d). As seen in the ternary plot of Th-Hf/3-Nb/16 (Wood, 1980), samples plot in the field of calcalkaline volcanic arc basalts (Figure 19a). Agrawal et al. (2008) used trace elements that are easily mobilised in low alteration and metamorphism conditions (La, Sm, Yb, Nb and Th) to determine the tectonic environment of basic and ultrabasic rocks (island arc, continental rift, oceanic island and mid-ocean ridge). On this tectonic discrimination diagram, the Pazarcık volcanics and Yaycılar gabbro cluster in the island arc basalt field (Figure 19b).

Figure 19c shows the Th/Yb versus Ta/Yb diagram of Pearce (1983). Accordingly, samples from the Pazarcık and Kiremitlik volcanic members and Yaycılar gabbro are plotted within the volcanic arc field (Figure 19c). Although the Pazarcık volcanic member and Yaycılar gabbro fall in the calc-alkali series, the Kiremitlik volcanic member samples cluster in the shoshonitic field. In the tectonic discrimination diagram (Figure 19d) of Thieblemont and Tegyey

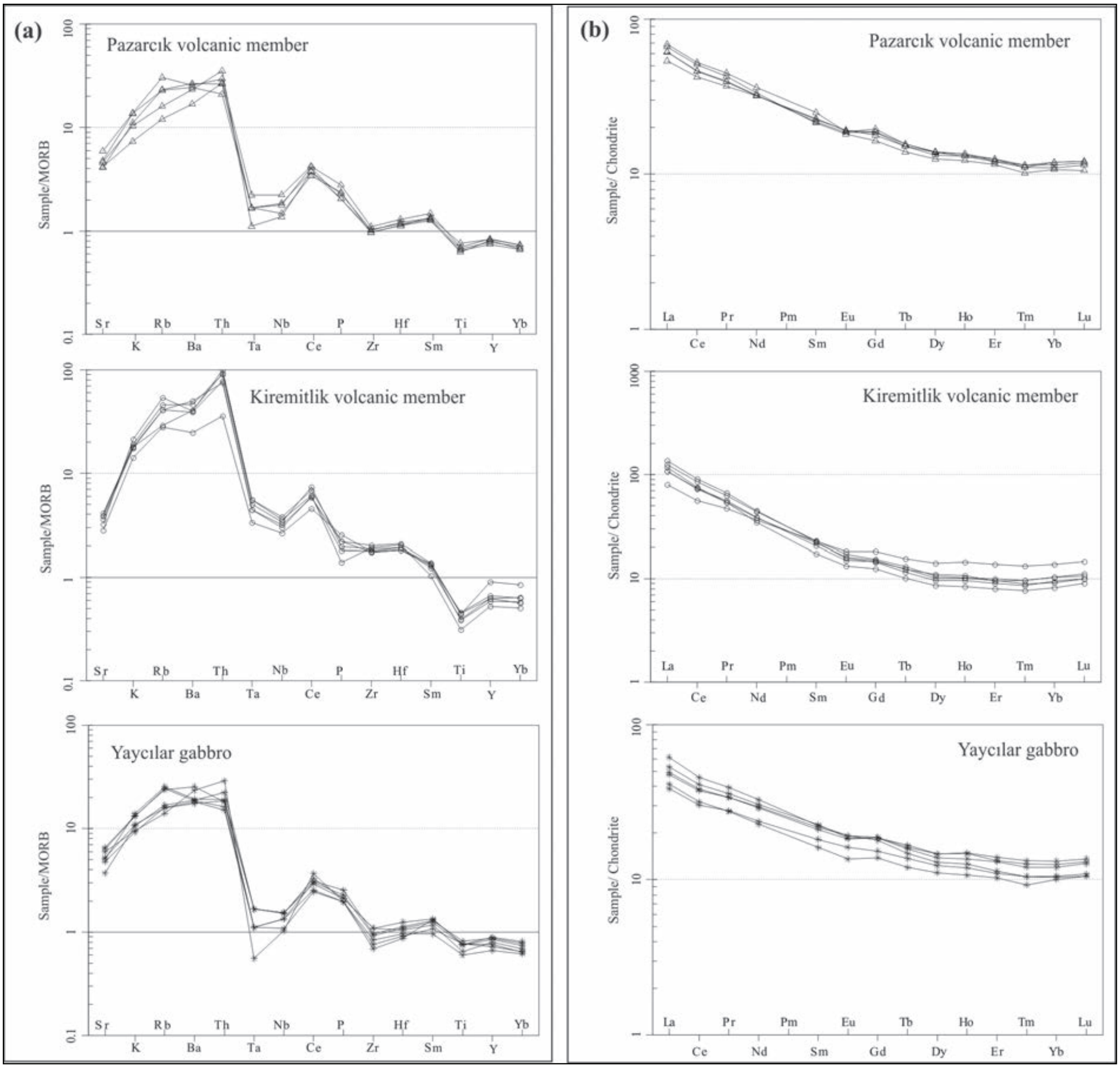

Figure 17- (a) MORB (Pearce, 1983) and (b) Chondrite-normalised (Boynton, 1984) multi-element distribution diagrams of Pazarcık and Kiremitlik volcanic members and Yaycılar Gabbro.

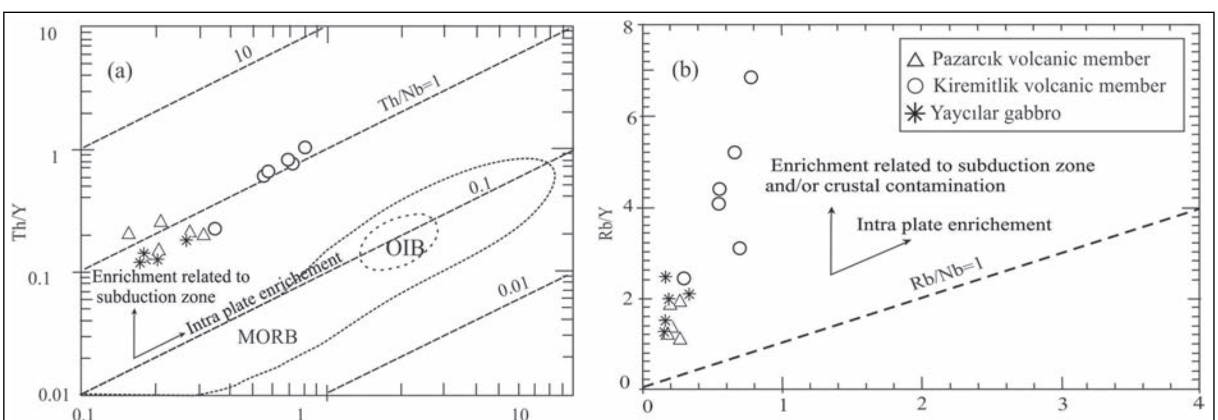

Figure 18- (a) Nb/Y vs. Th/Y (Pearce, 1983) and (b) Nb/Y vs. Rb/Y (Edwards et al., 1991) diagrams of Pazarcık and Kiremitlik volcanic members and Yaycılar Gabbro.

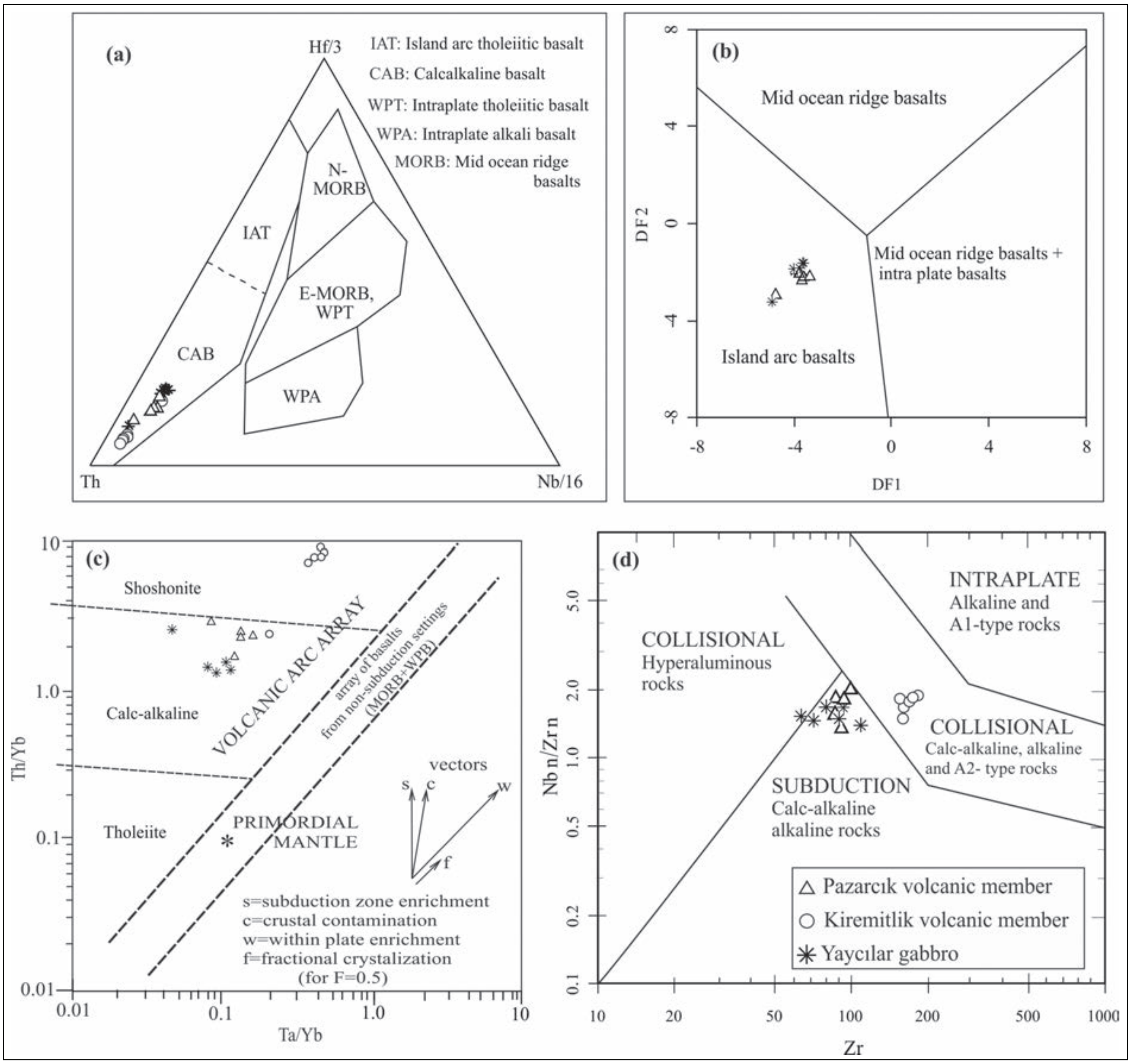

Figure 19- Tectonic discrimination diagrams for Pazarcık and Kiremitlik volcanics (a) Th-Hf/3-Nb/16 ternary diagram of Wood (1980), (b) DF1 vs. DF2 diagram of Agrawal et al. (2008), (c) Th/Yb vs Ta/Yb discrimination diagram of Pearce (1983 and (d) Zr vs. Nb_n/Zr_n diagram of Thieblemont and Tegyey (1994). [DF1= 0.3518*ln(La/Th)+0.6013*ln(Sm/Th)-1.3450*ln(Yb/Th)+2.1056*ln(Nb/Th)-5.4763; DF2= 0.3050*ln(La/Th)-1.1801*ln(Sm/Th)+1.6189* ln(Yb/Th)+1.226* ln(Nb/Th)-0.9944].

(1994), Pazarcık volcanic member and Yaycılar Gabbro are located in the field related to subduction, whereas samples from the Kiremitlik volcanic member fall in the field related to collision (Figure 19d).

In this study, it is considered that the Pazarcık volcanic member was derived from a mantle source metosomatised by subduction zone components. The Kiremitlik volcanic member was derived from a mantle source at the base of continental lithosphere metasomatised by subduction events which evolved with partial melting during the slab breakoff process occurring in the late stage of collision.

5. Geologic Evolution of Sorgun-Yıldızeli Basin and Discussion

The geologic, sedimentologic, petrographic and geochemical data obtained in this study indicate the Sorgun-Yıldızeli basin is an east-west oriented asymmetric foreland basin. It developed along the northern edge of the Kırşehir Block, above the remnants of the Izmir-Ankara-Erzincan Suture Zone during the subduction of oceanic crust belonging to the northern branch of Neotethys and the collision of the Sakarya continent to the north with the Kırşehir Block to the south.

In light of data obtained from the Sorgun-Yıldızeli foreland basin, an attempt is made to explain the evolution of the basin under the following headings; pre-collisional period (pre-Maastrichtian), collision period (late Maastrichtian-early Palaeocene (early stage) and late Palaeocene-early Lutetian (late stage) periods) and post-collisional period (Lutetian-late Eocene).

5.1. Pre-Collision Period (Pre-Maastrichtian)

During this period, the floor of the Neotethys ocean began to descended under the Sakarya continent to the north beginning in the Cenomanian (Tüysüz and Dellaloğlu, 1992; Tüysüz et al., 1995). Consumption of the oceanic crust of the northern branch of Neotethys occurred in two different subduction events according to Tüysüz and Dellaloğlu (1992) and Tüysüz et al. (1995). The first of these produced an ensialic arc on the Sakarya continent (Andes-type active continental margin volcanic belt), while the second was intraoceanic subduction producing an ensimatic island arc (Figure 20).

5.2. Collisional Period

5.2.1. Late Maastrichtian-Early Palaeocene (Early Stage)

According to Keskin et al. (2008), toward the end of the Maastrichtian the Kırşehir Block to the south and the Sakarya continent to the north were close enough to initiate collision. Due to the irregularity of the partly colliding continental margins, deposition continued in remnant basins along the collision zone. For example, the remnant basin where the Hıdırnalı group was deposited located south of Tokat (Yılmaz et al., 1993; 1997) continued to experience marine sedimentation until the beginning of the Lutetian.

Our observations in areas where the Hıdırnalı group outcrops (for correlation of sedimentologic and structural characteristics with the Sorgun-Yıldızeli basin) indicate that this remnant basin transformed into a foreland basin from the late Palaeocene in similar to that of the Sorgun-Yıldızeli basin (Figure 21 a,b).

5.2.2.Late Palaeocene-Early Lutetian Period (Late Stage)

Due to continuing N-S oriented compression, the accretionary complex was sliced, overthrust and formed an imbricated structure, causing thickening of the accretionary complex in this period. As a result of continued subduction of oceanic crust and dragging under of the Kırşehir Block, remnant basins along the collision zone were severely narrowed and experienced deformation. From the late Palaeocene period they were transformed into east-west oriented asymmetric margin foreland basins.

Deposition of the Dolak member represented by olistoliths and slices belonging to the accretionary complex along the northern margin of the Sorgun-Yıldızeli foreland basin, alluvial fan and fan delta sediments, continued during the late Palaeocene-middle Eocene period. Olistoliths of varying sizes belonging to the accretionary complex are present within the unit and, slices and thrust plates of ophiolite show that intense compression and shortening was effective during basin development (Figure 22a).

While basin deposition continued in the late Palaeocene-early Eocene period, basaltic lava and pyroclastics of Pazarcık volcanic member carrying subduction signatures, formed in the basin (Figure 22b).

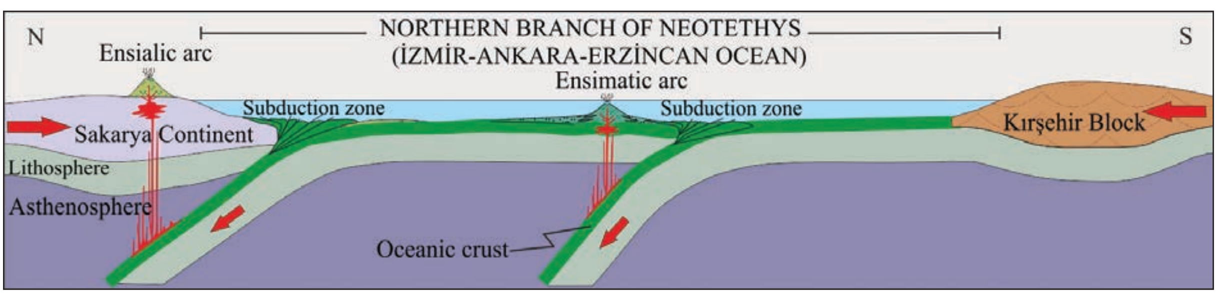

Figure 20- Model section showing tectonic evolution of the northern branch of the Neotethys ocean in the pre-Maastrichtian period (adapted from Tüysüz and Dellaloğlu, 1992).

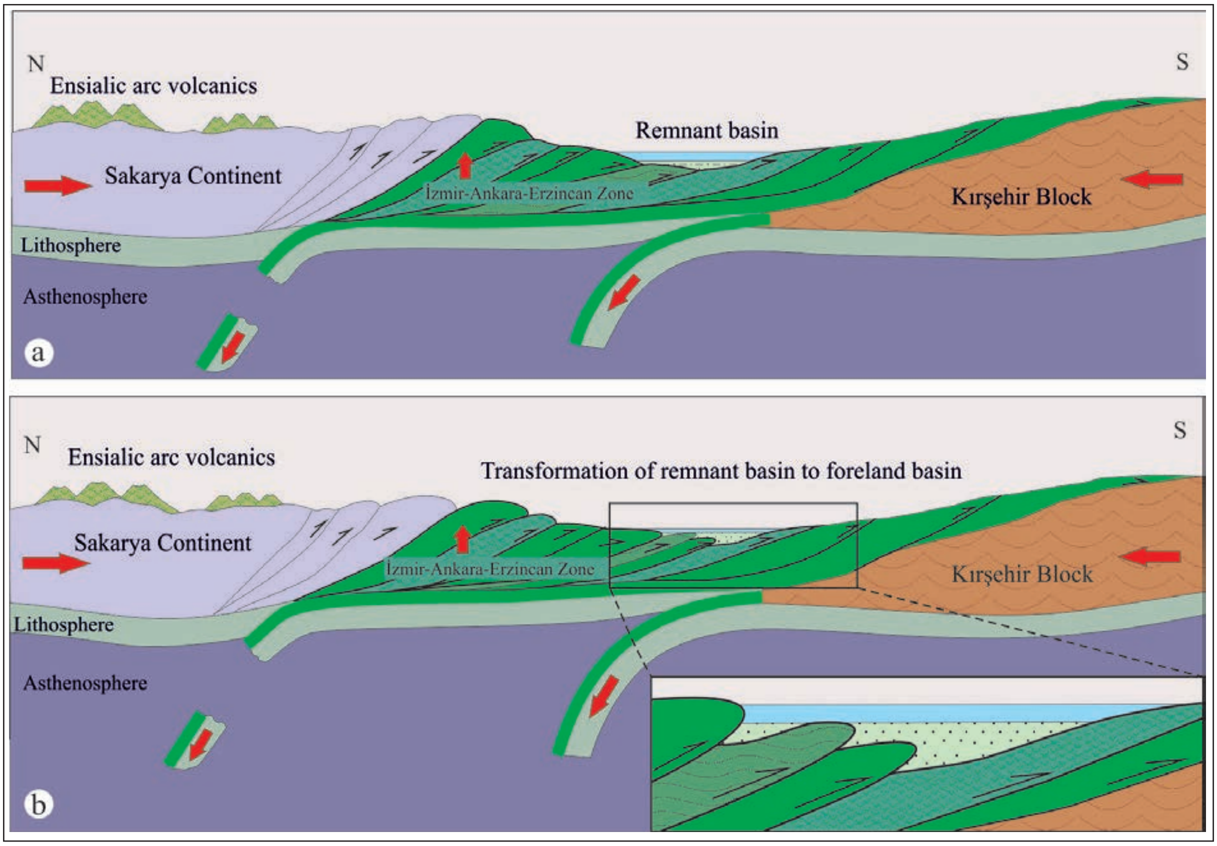

Figure 21- Model section showing tectonic evolution of the northern branch of the Neotethys ocean in (a) Late Maastrichtian-Early Palaeocene and (b) Late Palaeocene.

These volcanics were interpreted by Alpaslan (2000) as due to low-degree partial melting of the upper mantle in an extensional tectonic regime formed in the region in the stage following collision between the Pontides and Anatolides or as products of intraplate magmatism after collision by Koçbulut et al. (2001). In this study, the Pazarcık volcanics are interpreted as products of subduction-related magmatism formed in a compressional tectonic regime.

The Yaycılar gabbro exhibiting similar geochemical characteristics to the Pazarcık volcanics, was emplaced in basal sections of the Boğazköy Formation as sills and laccoliths (Figure 22c).

In the early-middle Eocene period, the composition of volcanism changed from basic to acidic and as a result, Sarayözü dacite and rhyolite volcanic member was formed (Figure 22d). This compositional change in volcanism may have developed as a result of different mechanisms such as differentiation and fractional crystallisation processes in the evolution of magmas, variable degrees of partial melting or partial melting due to dehydration reactions of crustal rocks as a result of emplacement of basic magma into the lower sections of the continental crust.

In the late stage of collision in the middle Eocene, slab breakoff related to collision was accompanied by emplacement of the Kiremitlik volcanics comprising andesitic lava and pyroclastic rocks (Figure 22e).

The Kiremitlik volcanic member is considered to have derived from a mantle source that evolved as a result of partial melting of the base of the continental lithosphere. This lithosphere had been metasomatised by subduction events due to heat transfer to the continental lithosphere linked to the slab breakoff mechanism.

A study by Keskin et al. (2008) of the western continuation of the study area in the Amasya-Çorum area proposed that volcanism in the middle Eocene developed as a result of slab breakoff. According to this model, with the final closure of remnant basins along the collision zone, sedimentation continued in the Çankırı basin during the Eocene, the suture zone elevated above sea level and experienced significant

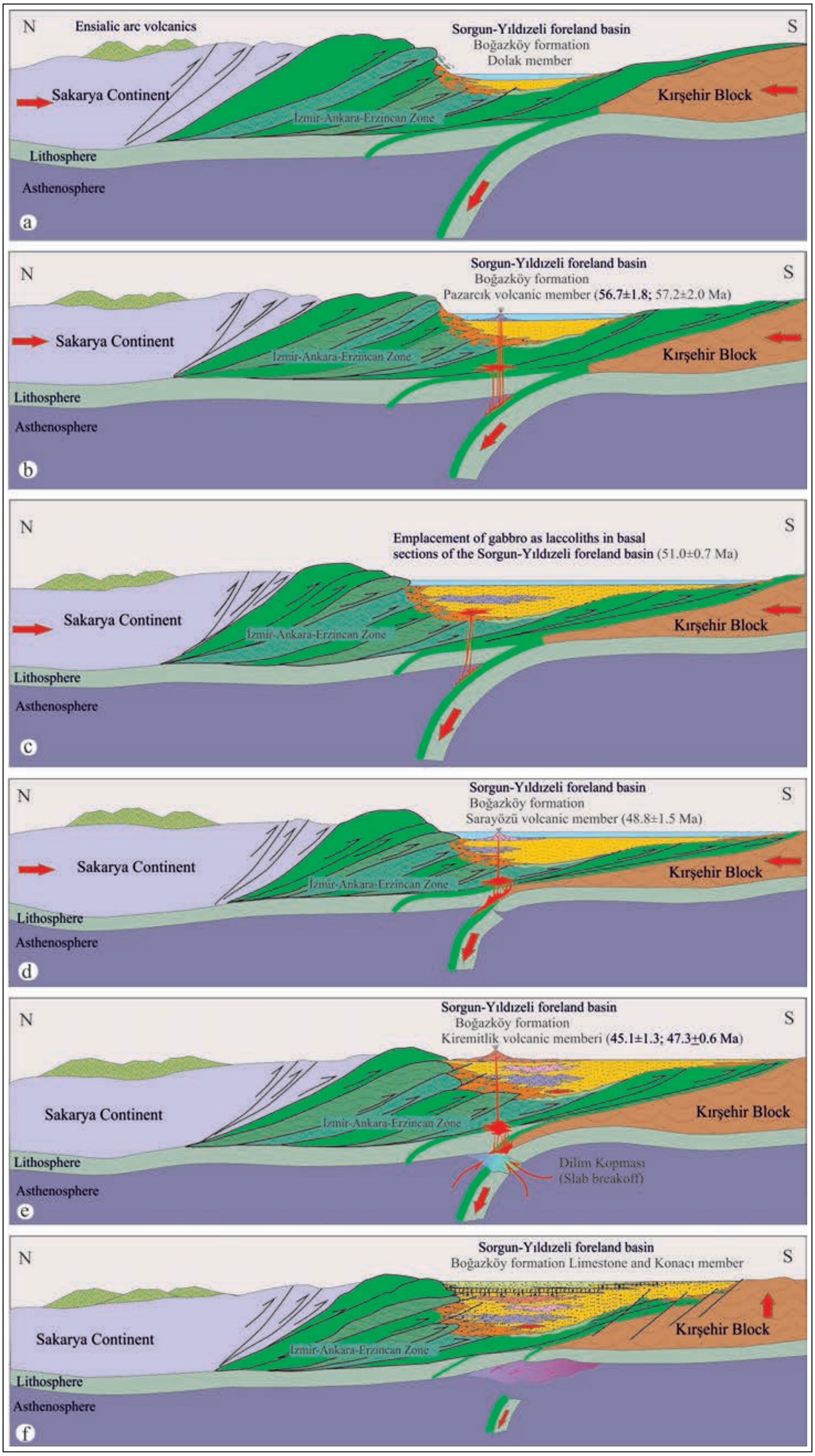

Figure 22- Model section showing tectonic evolution of the Sorgun-Yıldızeli foreland basin in the Late Palaeocene-Early Lutetian period.

erosion until the end of the early Eocene. Beneath the collision zone, with the slab pull of the oceanic lithosphere representing the northern Neotethys ocean controlling the basin, the region became a shallow marine environment with a new transgression in the Lutetian.

Kaymakçı et al. (2009) interpreted the Çankırı basin as a part of a fore-arc basin in terms of location in the Late Cretaceous and stated that a series of piggy-back basins developed above in the Paleocene and later periods with forearc sequences deposited in southward depositional environments.

According to the model recommended in this study, with the remnant basins along the collision zone between the Sakarya continent to the north and the Kırşehir Block to the south experiencing deformation in the late Palaeocene and transformation into foreland basins, though some sections were covered by younger units, not only the Çankırı basin but the eastern extension of this basin of the Çorum, Yozgat, Sorgun and Yıldızeli basins continued sedimenting into the early Lutetian period. Due to relaxation after slab breakoff in the Lutetian, the Kırşehir Block began to be uplifted, the Sorgun-Yıldızeli foreland basin shallowed significantly and the Limestone member comprising reefal limestones and the Konacı member consisting clastic rocks with claystone and clayey limestone layers were deposited (Figure 22f).

5.3. Post-Collisional Period (Lutetian-Early Eocene)

During the rapid uplift and relaxation of the Kırşehir Block as a result of slab breakoff in the Lutetian under control of an extensional tectonic regime above the regressive foreland basin and basement rocks, after collision transgressive basins developed (Figure 23a).

The slab breakoff event was effective in transforming the compressional tectonic regime characterised by thrust faulting that dominated until the Lutetian period into an extensional tectonic regime with normal faulting effective in the Lutetian.

The middle-late Eocene Tokuş Formation, comprising the basal conglomerate Susuzdağ member was deposited unconformably above the Akdağmadeni Massif and Boğazköy Formation in a post-collisional basin. The alluvial fan and fan delta sediments of Susuzdağ member pass laterally and vertically into sandstone, sandy limestone, claystone, shale and Nummulites limestone of the Tokuş Formation (Figure 23c).

These post-collisional basins representing the Lutetian-late Eocene period contain volcanic products with characteristics partly similar to the volcanics in the foreland basins as they evolved during the late Palaeocene-early Lutetian period. According to the model proposed in this study, the foreland basins contain volcanic rocks related to subduction processes before slab breakoff and to collision developing during the slab breakoff process. In contrast, post-collisional basins formed in the middle-upper Eocene period contain volcanic rocks related to partial melting of continental lithosphere metasomatised by previous subduction events which hot asthenosphere filled the broken slab volume and magma chambers were emplaced in different sections of the continental crust. Near Ortaköy in the study area, the basal conglomerates of the Tokuş Formation (Susuzdağ member) and the interleaved acidic composition lava and pyroclastic rocks (Ortaköy volcanics) may have developed as a result of this type of mechanism (Figure 23b).

6. Conclusions

The rock assemblages that were apparently deposited in two separate E-W oriented basins between Sorgun (Yozgat) and Yıldızeli (Sivas) were determined to be products of a single large basin developed as a result of the same geodynamic processes ("Sorgun-Yıldızeli basin").

The Sorgun-Yıldızeli basin developed as an east-west oriented asymmetric margin foreland basin accompanied by volcanism related to subduction and/or collision in the late Palaeocene-middle Eocene period during the process of consumption of oceanic crust of the northern branch of Neotethys and the collision of the Sakarya continent to the north with the Kırşehir Block to the south.

The basin fill consists mainly of the Boğazköy Formation and its differentiated subunits. In the basal section of this formation, gabbroic sills and laccoliths, emplaced at shallow depths are called the Yaycılar gabbro.

Interspersed with sedimentary rocks within the basin are also basalt, basaltic andesitic composition lava and pyroclastics of the Pazarcık volcanic member, dacite and rhyolite composition lava and pyroclastics of the Sarayözü volcanic member and andesite and trachyandesite composition lava and pyroclastics of the Kiremitlik volcanic member.

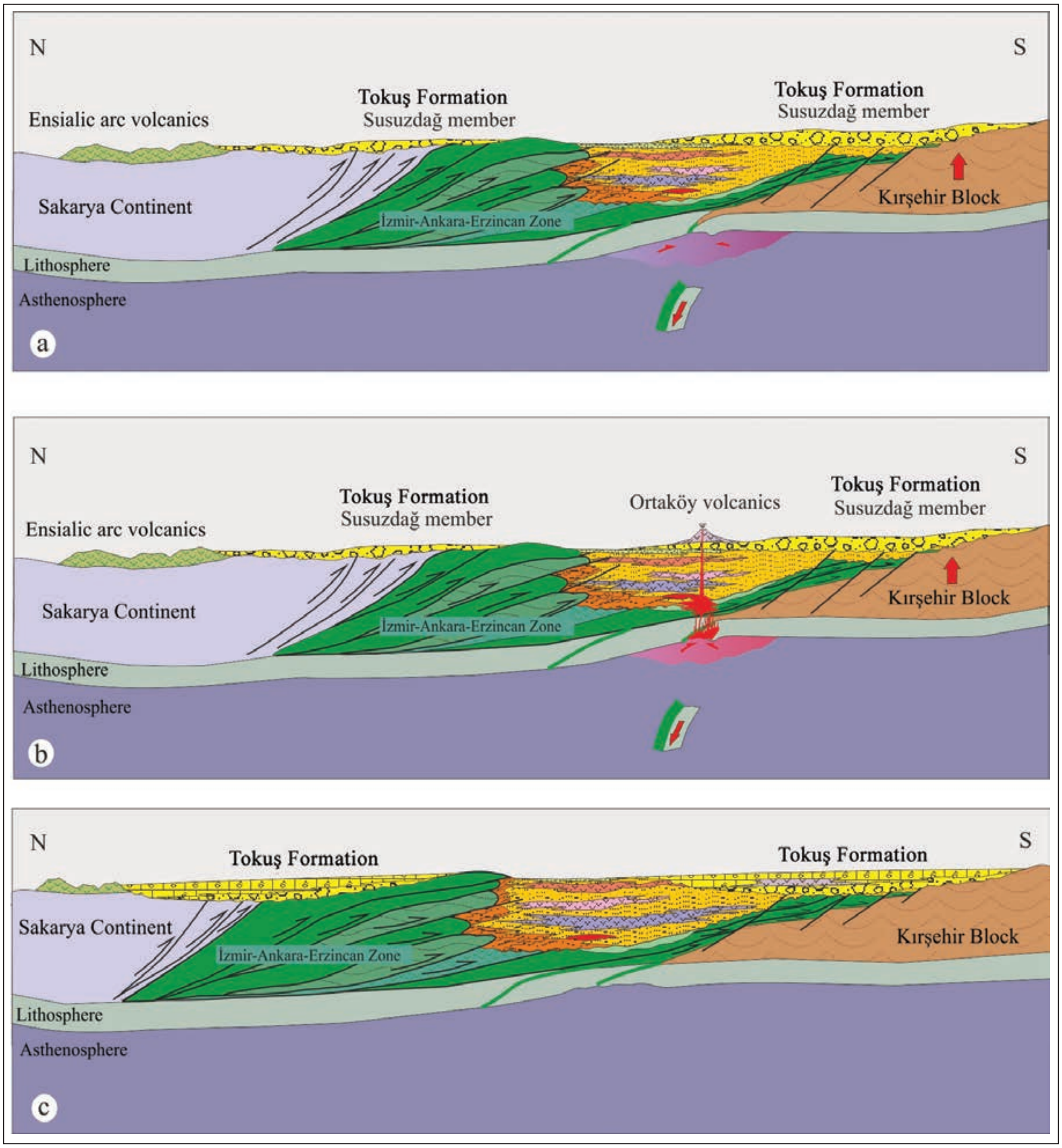

Figure 23- Model section showing tectonic evolution of post-collisional basin (Lutetian-Late Eocene period).

Based on geochemical data, together with multi-element distribution and tectonic discrimination diagrams, the Pazarcık volcanic member may be interpreted as a product of calcalkaline character volcanism related to active subduction in the late Palaeocene-early Eocene period (57.2±2.0 My and 56.7±1.8 My). Yaycılar gabbro (51.0±0.7 My) exhibiting similar geochemical features to that of Pazarcık volcanics is the product of subduction-related magmatism. The Kiremitlik volcanic member (45.1±1.3 Ma and 47.3±0.6 Ma) is interpreted as the product of calcalkaline character volcanism related to collision and developed during the slab breakoff process in the middle Eocene.

Rapid uplift of the Kırşehir Block due to slab breakoff occurring in the Lutetian led to development of transgressive post-collisional basins over the regressive foreland basin and basement rocks under control of an extensional tectonic regime, with volcanic activity continuing in these basins.

The basal conglomerate (Susuzdağ member) of the Tokuş Formation comprising post-collisional basin fill around Ortaköy and the interfingering with the acidic composition lava and pyroclastic rocks of the Ortaköy volcanics are interpreted as a product of post-collisional volcanism effective after slab breakoff.

Acknowledgements

This study includes a portion of the findings obtained during the "Geology and Geodynamic evolution process of the Akdağmadeni Massif" organised by the Directorate of Geological Studies of the General Directorate of Mineral Research and Exploration (MTA). Whole rock geochemical analyses and $^{40}Ar/^{39}Ar$ geochronologic age dating was performed in ActLabs Canada. Petrographic identification of samples was completed by Geo. Eng. (MS) Asuman Besbelli, Dr. Nihal Görmüş, Geo. Eng. Sema Çobankaya, and Geo. Eng. (MS) Ezgi Ulusoy, and palaeontologic dating was performed by Dr. Erkan Ekmekçi, Dr. Aynur Hakyemez, Dr. Fatma Gedik, Geo. Eng. (MS) Ayşegül Aydın and Geo. Eng. (MS) Dilek Tokatlı. Firstly, we would like to thank the department of Geological Research of the General Directorate of Mineral Research and Exploration and Prof.Dr. Ali Yılmaz, Geo. Eng. Mustafa Dönmez, Geo. Eng. (MS) Sibel Karacadoğan and Geo. Eng. Halil Keskin for their constructive reviews and contributions to the preparation of the publication. Additionally, we thank the reviewers Prof. Dr. Ş. Can Genç, Prof. Dr. Orhan Tatar and Prof. Dr. Faruk Aydın for detailed reviews and beneficial and important criticism which improved the first draft.

References

Agrawal, S., Guevara, M., Verma S. 2008. Tectonic discrimination of basic and ultrabasic volcanic rocks through log-transformed ratios of immobile trace elements. International Geology Review 50, 1057–1079.

Akçay, A. E., Dönmez, M., Kara, H., Yergök, A. F., Esentürk, K. 2008. 1/100.000 Ölçekli Türkiye jeoloji haritaları, Kırşehir sheet İ-34, No: 81. General Directorate of the Mineral Research and Exploration, Ankara.

Aldanmaz, E., Pearce, J., Thirhvall, M.F., Mitchell, J. 2000. Petrogenetic evolution of late Cenozoic, post-collision volcanism in western Anatolia, Turkey. Journal of Volcanology and Geothermal Research 102, 67-95.

Alpaslan, M. 2000. Pazarcık volkanitinin (Yıldızeli-Sivas) mineralojik-petrografik ve jeokimyasal özellikleri. Türkiye Jeoloji Bülteni 43/2, 49-60.

Alpaslan, M., Terzioğlu, N. 1998. Pontidlerde çarpışma sonrası volkanizmaya bir örnek: Sürmeli Volkaniti (Taşova-Amasya), CÜ Mühendislik Fakültesi Dergisi, Seri A: Yerbilimleri, 15, 1, 13-20.

Altunkaynak, Ş. 2007. Collision-driven slab breakoff magmatism in northwestern Anatolia, Turkey. Journal of Geology 115, 63-82.

Altunkaynak, Ş., Dilek, Y. 2006. Timing and nature of postcollisional volcanism in western Anatolia and geodynamic implications. In: Postcollisional Tectonics and Magmatism in the Mediterranean Region and Asia, Y. Dilek and S. Pavlides (eds.), Geological Society of America, Special Paper, 409, 321-351.

Altunkaynak, Ş., Dilek, Y. 2013. Eocene mafic volcanism in northern Anatolia: its causes and mantle sources in the absence of active subduction. International Geology Review 55 (13), 1641-1659.

Arslan, M., Aliyazıcıoğlu, İ. 2001. Geochemical and petrological characteristics of the Kale (Gümüşhane) volcanic rocks: Implications for the Eocene evolution of Eastern Pontide arc volcanism, Northeast Turkey, International Geology Review 43, 595-610.

Atakay Gündoğdu, E. 2009. Çorum Güneybatısındaki Volkanik Kayaçların Jeolojik Ve Petrolojik Özellikleri ve Alaca Höyük Kazısında Jeoarkeolojik Çalısmalar, PhD Thesis, Institute of science, Ankara Universty,194p. (unpublished).

Bailey, E.B., Mc Callien, W.J. 1950. Ankara melanjı ve Anadolu şariyajı. Maden Tetkik ve Arama Dergisi 40, 12-16.

Beyazpirinç, M., Akçay, A.E., Tarhan, N., Sönmez, M.K., Havzoğlu, T., Bilgiç, T., Bademler, F., Ünal, M. 2014. Akdağmadeni masifinin jeolojisi ve jeodinamik evrimi projesi 2011-2012 yıllarına ait ara rapor. General Directorate of Mineral Research and Exploration Report No: 11763, Ankara (unpublished).

Boynton, W. V. 1984. Cosmochemistry of the rare earth elements: meteorite studies. In: Henderson P (eds) Rare Earth Element Geochemistry. Elsevier, Amsterdam, 63-114.

Büyükönal, G. 1985. Distribution of the major and trace elements in the volcanic rocks of Yozgat area, Turkey. Bulletin of the Mineral Research and Exploration 105-106; 68-82.

Dalkılıç, H., Dönmez, M., Akçay, A. E. 2008. 1/100 000 Ölçekli açınsama nitelikli Türkiye Jeoloji Haritaları Serisi, Yozgat-Sheet İ35, No: 82. General Directorate Mineral Research and Exploration, Ankara.

Debon, F., Le Fort, P. 1983. A chemical–mineralogical classification of common plutonic rocks and associations. Transactions of the Royal Society of Edinburgh, Earth Sciences 73, 135–149.

Dilek, Y., Thy, P. 2006. Age and petrogenesis of plagiogranite intrusions in the Ankara melange, Central Turkey. Island 15, 44-57.

Dönmez, M., Bilgin, Z.R., Akçay, A.E., Kara, H., Yergök, A.F., Esentürk, K. 2005. 1/100.000 Ölçekli açınsama nitelikli Türkiye Jeoloji Haritaları Serisi, Kırşehir Sheet İ31 , No: 46. General Directorate of Mineral Research and Exploration, Ankara.

Dönmez, M., Akçay, A.E., Genç, Ş.C., Acar Ş. 2005. Biga yarımadasında Orta-Üst Eosen volkanizması ve denizel ignimbiritler, Maden Tetkik ve Arama Dergisi 131, 49-61.

Edwards, A., Menzies, M., Thirlwall, M. 1991. Evidence from Muriah, Indonesia, for the interplay of supra-subduction zone and intraplate processes in the genesis of potassic alkaline magmas. J.Petrol., vol. 32(3), p.555-592.

Egeran, E.N., Lahn, E. 1951. Kuzey ve Orta Anadolu’nun tektonik durumu hakkında not. Maden Tetkik ve Arama Dergisi 41, 23-27.

Ercan, T., Ergül, E., Akçören, F., Çetin, A., Granit, S., Asutay, J. 1990. Balıkesir-Bandırma arasının jeolojisi, Tersiyer volkanizmasının petrolojisi. Maden Tetkik ve Arama Dergisi 110, 113-30.

Ercan, T., Satır, M., Steinitz, G., Dora, A., Sarıfakıoğlu, E., Adis, C., Walter, H.-J., Yıldırım, T. 1995. Biga yarimadasi ile Gökceada, Bozcaada ve Tavsan adalarindaki (KB Anadolu) Tersiyer volkanizmasinin ozellikleri. Maden Tetkik ve Arama Dergisi 117, 55-86.

Ercan, T., Türkecan, A., Guillou, H., Satır, M., Sevin, D., Şaroğlu, F. 1998. Marmara denizi çevresindeki Tersiyer volkanizmasının özellikleri. Maden Tetkik ve Arama Dergisi 120, 199–221.

Erkan, Y., Ataman, G. 1981. Orta Anadolu masifi (Kırşehir yöresi) metamorfizma yaşı üzerine K-Ar yöntemi ile bir inceleme. Yerbilimleri 8, 27-30.

Erler, A., Bayhan, H. 1995, Orta Anadolu granitoyitlerinin genel değerlendirilmesi ve sorunları. Yerbilimleri 17, 49-67.

Fitton, J.G., James, D., Kempton, P.D., Ormerod, D.S., Leeman, W.P. 1988. The role of lithospheric mantle in the generation of late Cenozoic basic magmas in the Western United States, Journal of Petrology, Special Issue, 331-349.

Genç, Ş.C. 1998. Evolution of the Bayramiç magmatic complex. Journal of Volcanology and Geothermal Research 85 (1-4), 233-249.

Genç, Ş.C., Yılmaz, Y. 1997. An example of post-collisional magmatism in northwestern Anatolia: the Kızderbent volcanics (Armutlu peninsula, Turkey). Turkish Journal of Earth Sciences 6, 33–42.

Genç, Ş.C., Dönmez, M., Akçay, A., Altunkaynak, Ş. 2004. The Middle Eocene to Late Miocene magmatic evolution of the Biga peninsula, NW Turkey. 32nd International Geological Congress, Florence, Italy, Abstracts Part 2, 1298.

Genç, Ş.C., İşseven, T., Keskin, M., Tüysüz, O. 2005. Armutlu yarımadası (KB Anadolu) Eosen magmatik kayalarının petrolojik evrimi ve paleomanyetizma özelliklerinin araştırılması. TÜBİTAK Projesi (Proje No: 102Y032).

Genç, Ş.C., Altunkaynak, Ş. 2007, Eybek graniti (Biga yarımadası, KB Anadolu) üzerine: yeni jeokimya verileri ve yeni bir değerlendirme. Hacettepe Universitesi Yerbilimleri Uygulama ve Araştırma Merkezi Dergisi 28 (2), 75-98.

Gill, J.B. 1981, Orogenic andesites and Plate tectonics, Springer - Verlag, New York, 138 p.

Göncüoğlu, M.C. 1977. Geologie des westlichen Niğde Massivs. Univ. Bonn, Ph.D. Thesis, 181 p. (unpublished).

Göncüoğlu, M.C.,Toprak, V., Kuşçu, I., Erler, A., Olgun, E. 1991. Orta Anadolu Masifi’nin batı bölümünün jeolojisi, Bölüm 1: Güney Kesim. TPAO Rapor No: 2909, 140 p. (unpublished).

Göncüoğlu, M.C., Erler, A., Toprak, V., Yalınız, K., Olgun, E., Rojay, B. 1992. Orta Anadolu Masifi’nin batı bölümünün jeolojisi, Bölüm 2: Orta Kesim. TPAO Rapor No: 3155, 76 p. (unpublished).

Görür, N., Akkök, R., Sakınç, M., Ünalan, G., Yaltırak, C. 1997, Türkiye’nin Tersiyer Havzaları ve Kömür Potansiyeli. Türkiye Kömür Arama Hedeflerinin Belirlenmesi ve Arama Yöntemlerinin Saptanması, Yurt Madenciliğini Geliştirme Vakfı Yayınları, s. 8-37.

Gülmez, F., Genç, S.C., Keskin, M., Tüysüz, O. 2013. A postcollision slab-breakoff model for the origin of the Middle Eocene magmatic rocks of the Armutlu-Almacık belt, NW Turkey and its regional implications, in Robertson, A.H.F., Parlak, O., and Ünlügenç, U.C., eds., Geological development of Anatolia and the Easternmost Mediterranean region: Geological Society, London, Special Publications, 372.

Kara, H. 1997. 1/100.000 ölçekli açınsama nitelikli Türkiye jeoloji haritaları serisi, Yozgat G 19 paftası, No. 54. Maden Tetkik ve Arama Genel Müdürlüğü, Ankara.

Kaymakçı, N., Özçelik, Y., White, S.H., Van Dijk, P.M. 2009. Tectono-stratigraphy of the Çankırı Basin: Late Cretaceous to Early Miocene evolution of the Neotethyan Suture Zone in Turkey. Geological Society, London, Special Publications 311, 67–106.

Keskin, M., Genç, S.C., Tüysüz, O. 2004. Tectonic setting and petrology of collision-related Eocene volcanism around the Çankırı Basin, North Central Turkey. 32nd IGC, Florence 2004 Abstracts Part 2, 1299.

Keskin, M., Genç, S.C., Tüysüz, O. 2008. Petrology and geochemistry of postcollisional Middle Eocene volcanic units in North-Central Turkey: Evidence for magma generation by slab breakoff following the closure of the Northern Neotethys Ocean. Lithos 104 (1-4), 267-305.

Ketin, İ. 1955. Yozgat bölgesinin jeolojisi ve Orta Anadolu Masifinin tektonik konumu. Türkiye Jeoloji Kurumu Bülteni 6, 1-40.

Ketin, İ. 1963. 1:500.000 ölçekli Türkiye Jeoloji Haritası (Kayseri). Maden Tetkik ve Arama Genel Müdürlüğü yayınları, 82 s. Ankara.

Ketin, İ. 1966. Anadolunun tektonik birlikleri, Maden Tetkik ve Arama Dergisi 66, 20-34

Koçbulut, F., Yılmaz Şahin, S., Tatar, O. 2001. Akdağmadeni (Yozgat)- Yıldızeli (Sivas) arasındaki Kaletepe volkanitinin mineralojik - petrografik ve jeokimyasal incelenmesi. İÜ Yerbilimleri Dergisi, Cilt 14, Sayı 1-2, 77-91.

Köprübaşı, N., Aldanmaz, E. 2004. Geochemical constraints on the petrogenesis of Cenozoic I-Type granitoids in Northwest Anatolia, Turkey: Evidence for magma generation by litospheric delamination in a post-collisional setting. International Geology Review 46, 705-729.

Le Bas, M.J., Le Maitre, R.W., Streckeisen, A., Zanettin, B. 1986. A chemical classification of volcanic rocks based on the total alkali-silica diagram. Journal of Petrology 27, 745–750.

Morrison, G.W. 1980. Characteristics and Tectonic Setting of the Shoshonite Rock Association. Lithos 13, 97-108.

Okay, A.İ., Tüysüz, O. 1999. Tethyan sutures of northern Turkey. In "The Mediterranean Basins: Tertiary extension within the Alpine orogen" (eds. B. Durand, L. Jolivet, F. Horváth and M. Séranne), Geological Society, London, Special Publication 156, 475-515.

Okay, A.İ., Satır, M. 2006. Geochronology of Eocene plutonism and metamorphism in northeast Turkey: evidence for a possible magmatic arc. Geodinamica Acta 19 (5), 251–266.

Özcan, A., Erkan, A., Keskin, E., Oral, A., Sümengen, M., Tekeli, O. 1980. Kuzey Anadolu fayı-Kırşehir masifi arasının temel jeolojisi. Maden Tetkik ve Arama Genel Müdürlüğü Rapor No:1604. Ankara (unpublished).

Pearce, J.A. 1983. Role of the sub-continental lithosphere in magma genesis at destructive plate margins. In: Hawkeswoeth, C.J. and Norry, M.J., (Eds), Continental basalts and Mantle Xenolithes. Nantwich: Shiva, 230-249.

Pearce, J. A. 1996. A user's guide to basalt discrimination diagrams. In: Wyman, D. A. (ed.) Trace Element Geochemistry of Volcanic Rocks: Applications for Massive Sulphide Exploration. Geological Association of Canada, Short Course Notes 12, 79–113.

Peccerillo, A., Taylor, S.R. 1976. Geochemistry of eocene calc-alkaline volcanic rocks from the Kastamonu area, northern Turkey. Contributions to Mineralogy and Petrology 58, 63-81.

Sarıfakıoğlu, E., Sevin, M., Esirtgen, E., Duran, S., Parlak, O., Bilgiç, T., Dönmez, M., Dilek, Y. 2011. Çankırı-Çorum havzasını çevreleyen ofiyolitik kayaçların jeolojisi: Petrojenezi, tektoniği ve cevher içerikleri. Maden Tetkik ve Arama Genel Müdürlüğü Rapor No: 11449, Ankara (unpublished).

Şahin, M.B. 1999. Akdağmadeni masifi metamorfitleri, Evciler-Çatköy kesiminin mineralojik ve petrolojik özelliklerinin incelenmesi. Doktora Tezi, HÜ Fen Bilimleri Enstitüsü, 105 s. Ankara (unpublished).

Şengör, A.M.C., Yılmaz, Y. 1981. Tethyan evolution of Turkey. A Plate Tectonic Approach. Tectonophysics 75, 181-241.

Terzioğlu, N. 1984. Ordu güneyindeki Eosen yaşlı Bayırköy volkanitlerinin jeokimyası ve petrolojisi, C.Ü. Mühendislik Fak. Dergisi, Seri-A Yerbilimleri, 1,43-60

Thieblemont, D., Tegyey, Y. 1994. Geochemical discrimination of differentiated magmatic rocks attesting for the variable origin and tectonic setting of calc-alkaline magmas. Comptes Rendus De L Academie Des Sciences Serie II 319 (1), 87–94.

Tiryaki, C., Ekici, T. 2012. Çarpışma sonrası kalk-alkalin Yozgat Volkaniklerinin Petrolojisi Türkiye Jeoloji Bülteni 55, 1

Tokel, S. 1972. Stratigraphical and Volcanic History of the Gümüşhane Region (NE Turkey), Doktora Tezi, Univ. Col. of London, UK.

Türkiye Stratigrafi Komitesi Bülteni, 1987, Sayı: 1, 15 s. Ankara.

Tüysüz, O., Dellaloğlu, A.A. 1992. Çankırı havzasının tektonik birlikleri ve jeolojik evrimi.Türkiye 9. Petrol Kongresi Kitabı, 333-349.

Tüysüz, O., Dellaloğlu, A.A., Terzioğlu, N. 1995. A magmatic belt within the Neo-Tethyan suture zone and its role in the tectonic evolution of Northern Turkey. Tectonophysics 243, 173-191.

Ustaömer P.A., Ustaömer T., Collins A.S., Reischpeitsch J. 2009. Lutetian Arc-Type Magmatism Along The Southern Eurasian Margin: New U-Pb La-Icpms And Whole-Rock Geochemical Data From Marmara Island, NW Turkey, Mıneralogy And Petrology 96, 177-196.

Vache, R. 1963. Akdağmadeni kontakt yatakları ve bunların Orta Anadolu Kristaline karşı olan jeolojik çerçevesi. Maden Tetkik ve Arama Dergisi 19, 22-36.

Whitney, D.L., Teyssier, C., Fayon, A.K., Hamilton, M.A., Heizler, M. 2003. Tectonic controls on metamorphism, partial melting and intrusion: timing and duration of regional metamorphism and magmatism in the Niğde Massif, Turkey, Tectonophysics, 376, 37-60

Wilson, M. 1989. Igneous Petrogenesis, Unwin Hyman Ltd., London, UK, 466p.

Winchester, J.A., Floyd, P.A. 1977. Geochemical classification of different magma series and their differentiation products using immobile elements. Chemical Geology 20, 325-343.

Wood, D.A. 1980. The application of a Th-Hf-Ta diagram to problems of tectonomagmatic classification and to establishing the nature of crustal contamination of basaltic lavas on the British Tertiary Volcanic Province: Earth and Planetary Science Letters, 50, 11-30.

Yılmaz, A. 1981. Tokat ile Sivas Arasındaki bölgede ofiyolitli karışığın iç yapısı ve yerleşme yaşı. Türkiye Jeoloji Kurumu Bülteni 24, 31-38

Yılmaz, A. 1982. Dumanlı dağı (Tokat) ile Çeltek dağı (Sivas)dolaylarının temel jeoloji özellikleri ve ofiyolitli karışığın konumu. Maden Tetkik ve Arama Genel Müdürlüğü Rapor No:7230, Ankara (unpublished).

Yılmaz, A., Uysal, Ş., Yusufoğlu, H., Ağan, A., inal, A., Aydın, N., Bedi, Y., Havzoğlu, T., Göç, D., İnal, E., Erkan, E.N. 1994. Akdağmasifi (Sivas) dolayının jeolojik incelemesi. Maden Tetkik ve Arama Genel Müdürlüğü Rapor No:9721, Ankara (unpublished).

YıImaz, A., UysaI, S, Bedi, Y., YusufoğIu, H., HavzoğIu, T., Ağan, A., Göç, D., Aydın, N. 1995. Akdağ masifi ve dolayının jeolojisi. Maden Tetkik ve Arama Dergisi 117, 125-138.

YıImaz, A., UysaI, S, Bedi, Y., Atabey, E.,YusufoğIu, H., HavzoğIu, T., Ağan, A., Aydın, N. 1997. 1/100.000 Ölçekli Türkiye jeoloji haritaları, Sivas-F22 paftası, No: 46. Maden Tetkik ve Arama Genel Müdürlügü, Ankara.

Yılmaz, Y., Gürpınar, O., Yiğitbaş, E.,Yıldırım, M., Genç, Ş.C., Gürer, Ö.F., Elmas, A., Bozcu, M.,Çalışkan, B.A. 1993. Tokat masifi ve yakın çevresinin jeolojisi. Türkiye Petrolleri Anonim Ortaklığı Rapor No: 3390.

Yılmaz, Y., Tüysüz, O., Yiğitbaş, E.,Genç, Ş.C., Şengör, A.M.C. 1997. Geology and tectonic evolution of the Pontides. In: Robinson, A.G. (Ed.), Regional and Petroleum Geology of the Black Sea and Surrounding Region. Memoir, vol. 68. American Association of Petroleum Geologists, pp. 183–226.

Yılmaz, Y., Tüysüz, O. 1984. Kastamonu-Boyabat-Vezirköprü-Tosya arasındaki bölgenin jeolojisi (Ilgaz-Kargı masiflerinin etüdü). Maden Tetkik Arama Enstitüsü Rapor No: 275, 275p

Yılmaz, Y., Genç, S.C., Karacık, Z., Altunkaynak, Ş. 2001. Two contrasting magmatic associations of NW Anatolia and their tectonic significance. Journal of Geodynamics 31, 243-271.

Bull. Min. Res. Exp. (2017) 155: 33-46

Bulletin of the Mineral Research and Exploration

http://bulletin.mta.gov.tr

TECTONIC GEOMORPHOLOGY OF BAŞKALE FAULT ZONE

Azad SAĞLAM SELÇUK[a*] and Meryem DÜZGÜN[b]

[a]Yüzüncü Yıl University, Faculty of Engineering-Architecture, Department of Geological Engineering, 65080 Tuşba/Van. orcid.org/0000-0003-4943-3870*

[b]Yüzüncü Yıl University, Institute of Science, 65080 Tuşba/Van. orcid.org/0000-0001-6017-2312

Research Article

Key words:
Başkale Fault Zone, Morphotectonic, geomorphic indices, uplift rates, the Eastern Anatolia.

Accepted Date: 10.07.2016
Received Date: 28.07.2016

ABSTRACT

Başkale Fault Zone is located between Şemdinli-Yüksekova fault zone in southeast Turkey and Guilato–Siahcheshmeh–Khoy fault system in southeast Iran. The fault zone started from Yavuzlar town to Işıklar village in southwest. BFZ is composed of three different segments which have directions with varying N75°E to N 80°E. The offset streams, fault controlled drainage system such as Çığılsuyu stream, alluvial fans which line up parallel to the fault and have deformation structure, fault straight, Plio-Quaternary volcanic rocks and volcanic structures, ridge travertines which continues their formations today indicate that BFZ is active as morphotectonic. The objective of the investigation is to determine the effect of Başkale Fault Zone on morphotectonic evolution of the region. With this aim, morphometric indices such hypsometric integral, drainage basin asymmetry, the ratio between the width and the height of valley and crimp in front of the mountain were produced with Digital Elevation Model of study area and were explained with their meaning. Depending on the results of morphometric models, it appears that the region has young topography and activelyrises. It was concluded that the rate of topographies rise in the region increased from east to west and typically rates were greater than of 0.5 mm in year.

1. Introduction

Başkale Fault Zone is located with the western section of the East Anatolia-Iran plateau forming the East Anatolia Compressional Tectonic Block (EACT). This block, defined by modeling of long-term GPS measurements (Reilinger et al., 2006; Djomour et al., 2011), is bounded by the left-lateral strike-slop Northeast Anatolian Fault in the northwest, by the Lesser Caucasus in the north/northeast and by the Bitlis-Zagros thrust belt in the south (Figure 1). It is proposed that the EACT developed under a N-S oriented compressional tectonic regime related to the continent-continent collision between the Arabian and Eurasian plate 13 million years ago (Şengör and Kidd, 1979; Şengör and Yılmaz, 1981; Dewey et al., 1986; Şaroğlu and Yılmaz, 1986; Yılmaz et al., 1987; Koçyiğit et al., 2001) (Figure 1). However, some studies published in recent years have stated that the tectonic regime represented by compression-shortening is only active along the Bitlis-Zagros thrust zone and between the end of the Late Miocene and end of the Early Pliocene (Koçyiğit et al., 2001; Koçyiğit, 2013). Koçyiğit et al. (2001) stated that instead of a compressional-shortening tectonic regime in the EACT block, a compressional type of neotectonic regime ended in the Late Pliocene. Linked to this regime, NW-SE and NE-SW oriented strike-slip faults, E-W oriented reverse/thrust faults and folds, N-S oriented normal faults and N-S oriented extensional fractures determining the location of significant volcanic centers developed in the region. Among the main neotectonic structures in the region are NW-SE oriented right-lateral strike-slip faults (Çaldıran (CF), Bitlis (BF) and Erciş (KEF) faults, etc.), NE-SW oriented left-lateral strike-slip faults (Ahlat fault (AhF), Başkale (BFZ) fault zone, etc.) and almost E-W oriented thrust faults (Muş-Gevaş thrust zone, Bitlis Zagros suture zone (BZSZ), Gürpınar fault (GF) and Van fault zone (TF) etc.) (Arpat et al., 1977; Şaroğlu et al., 1984; Koçyiğit, 1985*a*, 1985*b*;

* *Corresponding author: Azad Sağlam SELÇUK, azadsaglam@gmail.com*
http://dx.doi.org/10.19111/bulletinofmre.315757